Development of fluorine-free waterborne textile finishing agents for anti-stain and solvent-water separation based on low surface energy (co)polymers.

Amado Lacruz[a, c*], **Mireia Salvador**[a]

Miren Blanco[b], **Karmele Vidal**[b]

Antxon Martínez de Ilarduya[c]

[a] Color Center, S.A. Ptge. Marie Curie 3, Nau 6, 08223, Terrassa, Spain.

[b] Tekniker, Basque Research and Technology Alliance (BRTA), Surface Chemistry and Nanotechnology Unit, Iñaki Goenaga 5, 20600, Gipuzkoa, Spain.

[c] Departament d'Enginyeria Química, Universitat Politècnica de Catalunya, ETSEIB, Diagonal 647, 08028 Barcelona, Spain.

Abstract:

Fabric functionalization to obtain omniphobic textiles is an increasing trend due to science and technology push in our current society. Fluorochemicals dominate the water and oil-repellent textile finishing market because of their excellent performance. However, fluorinated chemicals release harmful substances giving rise to serious damage to ecosystems worldwide. In this paper, a series of fluorine-free, low surface energy and partially bio-based (co)polymethacrylates based on 3-[Tris(trimethylsilyloxy)silyl]propyl methacrylate (M3T) and stearyl methacrylate (SMA) have been successfully synthesized and characterized by Fourier-transform infrared spectroscopy (FTIR), nuclear magnetic resonance (NMR), differential scanning calorimetry (DSC), thermogravimetric analysis (TGA) and Energy-Dispersive X-ray Spectroscopy (EDS). Moreover, the particle size, particle size distribution and stability of developed emulsions have been assessed by laser diffraction spectrometry (LDS) and Z-potential measurements. The fluorine-free M3T/SMA (co)polymethacrylates have been applied on cotton fabrics by padding at several product dosages and coated textiles have been characterized by scanning electron microscopy (SEM), EDS element mapping, X ray fluorescence (XRF) and water and olive oil static contact angle measurements, WCA and OCA, respectively. Finally, performance of the fabrics treated with the new M3T/SMA (co)polymethacrylates has been evaluated and compared with textiles finished with conventional fluorinated chemicals. All the synthetized (co)polymethacrylates provide the coated substrates with high static water contact angles as well as excellent solvent-water separation efficiencies. However, only the textiles coated with the (co)polymethacrylates with higher M3T contents showed good repellence to olive oil, being able to keep the drop of oil on the surface for longer times. This time-dependent olive oil's wettability observed for the copolymers with low contents on M3T units may be ascribed to: i) the evolution with time of the surface free energy of the coatings due to a reorientation over time of stearyl side chains of SMA during contact with the olive oil; and ii) the reduced barrier properties of the coatings with lower content of the bulky tris(trimethylsilyloxy)silyl side chains.

Keywords: Anti-stain, Omniphobic, Fluorine-free, Solvent-Water separation, Technical textiles.

Amado Lacruz: Data Curation, Visualization, Project administration; Writing-Original draft preparation; Investigation
Miren Blanco: Conceptualization, Methodology, Writing- Original draft preparation
Mireia Salvador: Investigation, Resources, Visualization
Karmele Vidal: Investigation, Resources, Visualization
Antxon Martínez de Ilarduya: Writing - Review & Editing, Supervision

HIGHLIGHTS

- Fluorine-free waterborne (co)polymethacrylates for textile finishing are synthesized
- Polymer coatings are partially biobased, VOC-free and do not contain harmful chemicals
- Polymer coatings confer water-repellence and acceptable oil-repellence to fatty triglycerides
- Treated textiles have improved oil resistance due to tris-trimethylsilyloxy groups
- Treated textiles present excellent performance as a solvent-water separation membrane

---

* Corresponding Authors: Amado Lacruz (alacruz@colorcenter.es)
Phone number: +34 937861113

1. Introduction

Most textiles are manufactured from materials that have a remarkable wettability (cotton, silk, linen, polyester...) and therefore have a high tendency to absorb liquids. Modified textiles with treatments that give them hydrophobic and oleophobic properties are highly valued in textile industry not only on clothing, but also in technical textiles: medical fabrics, military uniforms and work protection, technical garments for extreme outdoor sports, textiles for public buildings, automotive, aeronautical, membranes for oil-water separation, etc. [1].

Currently, C8 fluorocarbons dominate the finishing agents' market, as they provide the fabrics with exceptional durable water and oil repellence (DWOR) properties as well as breathability. It is believed that the electronegativity of fluorine atom [2] and the orientation of the perfluorinated chains perpendicular to the textile fibres, helps the fabrics to form a "protective sheath" against fluids. Apart from the distribution of C8 fluorocarbons at surface and the generated roughness, low interchain forces, close pack of perfluorinated side chains of polymers and rigidity of the chains, contribute to their low surface energy that can reach values as low as 18 mN/m [3]. These finishing agents offer water contact angles of more than 150º and sliding angles of less than 10º, thus conferring superhydrophobicity, and also provide oil repellence (to a greater or lesser extent depending on the application dosage and the chemical structure of the fluorocarbon) [4-5]. However, despite their excellent performance, C8 fluorocarbons are a source of toxic chemicals that are released into the environment both in their manufacturing process (by-products) and subsequently, by degradation. These toxic substances, known as per- and polyfluorinated chemicals (PFCs), possess harmful effects on health and the environment. Some of them, such as perfluorooctanoic acid (PFOA) and perfluoroctane sulfonic acid (PFOS) are considered bioaccumulative compounds, suspected of being carcinogenic [6], they affect lipid metabolism, and also hormonal and reproductive systems [7-8], and are persistent in nature [9]. In 2000, the United States Environmental Protection Agency (EPA), aware of the scientific studies that pointed out that the PFOA was present in the blood of the entire world population [10], began leading actions for the progressive elimination of the PFOA (2010/15 Stewardship Program). The European community is also taking initiatives in this same direction, culminating in Regulation (EU) 2017/100032 that prohibits the manufacture and marketing of PFOA and related substances (including any polymer that has linear or branched perfluoroheptyl and/or perfluorooctyl groups) by the year 2020 (except for a few exceptions that have extensions).

The most logical alternative to replace C8 fluorocarbons (polymers containing lateral chains with 8 perfluorinated carbon atoms, also known as long-chain fluorocarbons) is the use of polymers with shorter perfluoroalkyl chains (from four to six perfluorinated carbons, also known as C4 and C6 fluorocarbons, respectively, or short-chain fluorocarbons generally speaking), that are not considered bioaccumulative [1,11-13]. However, short-chain fluorocarbons have comparatively lower mechanical and chemical resistance and worse performance [14] and therefore must be applied at higher doses. They have worse repellence to oils, and after a certain time, a drop of liquid ends up wetting the fabric. The Figure 1 explains the long-term wettability of the textiles treated with C8, C6 and C4 fluorocarbons. The low wettability of textile surfaces treated with C8 fluorocarbon is not a time-dependent mechanism while there is an increase in wettability over time as we move to short-chain fluorocarbons. The worse performance can be ascribed to the shorter length of the perfluorinated chains which, once in contact to the liquid drop, lose the ability to orient themselves perpendicularly to the fabric surface over time. In addition, C6 and C4 fluorocarbons generate PFCs, including perfluorohexanoic acid (PFHxA) and 1H, 1H, 2H, 2H -Perfluorooctanol (6:2 FTOH), which are currently under study to better understand their environmental and human health effects [5,15-16]. Fluorinated silicones and silanes are able to render oil-repellent surfaces but they fall in the same eco-toxicological drawbacks as fluorocarbons as far as they also have perfluorinated alkyl chains. All these concerns regarding fluorinated chemicals are leading to intensive research and high market demand of fluorine-free alternatives for DWOR finishing, as the textile industry lacks suitable alternatives with comparable material characteristics.

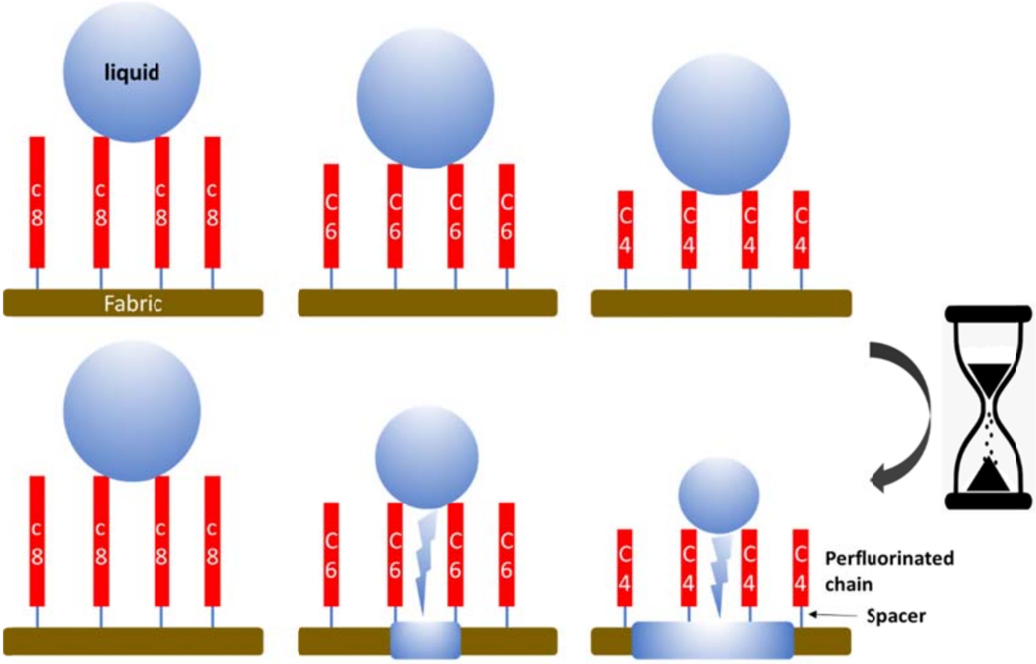

Figure 1. Long-term wettability of the textiles treated with C8, C6 and C4 fluorocarbons. Adapted from ref. [1]

The fluorine-free finishing agents explored in bibliography to achieve DWOR finishes are very diverse, based on very heterogeneous types of chemicals [1]. Fluorine-free long chain alkylamines [17], poly/mono-acrylates [18-19] or silicon containing monomers/polymers [20-23] are being highly studied as (super)hydrophobic finishing for textiles and are commonly blended with nanoparticles such as silica [18, 24-28], polydopamine nanoparticles [17, 29], Fe_3O_4 [30], TiO_2 [19, 31], montmorillonite [32] to achieve surface roughness and impart superhydrophobic properties in textile fabrics. Apart from polymeric hydrophobic treatments for textiles, fabrics coated with graphene oxides [33], water-repellent textiles obtained by plasma induced surface roughness [34], and textiles functionalized with nanoparticles with or without binding polymers [35] have been intensively investigated. Most of them provide complex approaches, which require several steps for their application on fabrics, which make them unattractive for their industrial implementation. The use of materials such as silanes or polysilsesquioxanes (POSS) with low availability and high price is also quite frequent, in addition to the use of solvents and additives with high environmental impact.

Among the explored alternatives, silicon-based polymers are becoming popular because fabrics treated with them exhibit low surface energy, water repellence, stain resistance, and they also confer high thermal stability as well as softness to the treated goods due to the flexibility of the Si-O-Si bonds. However, most silicon based polymers have poor mechanical properties and bad adhesion to the treated substrates. By contrast, acrylate polymers display good mechanical properties and good adhesion performance, but poor water resistance and thermal stability. In this context, many attempts for the preparation of silicon-containing acrylate polymers have been conducted with the aim of achieving positive synergies. Lei et al. [2] designed a series of copolymers by combining 3-[Tris(trimethylsilyloxy)silyl]propyl methacrylate (hereafter M3T) and different silicon-free (meth)acrylates to form copolymethacrylates with high silicon content. Side chain of M3T has three $Si\text{-}(CH_3)_3$ groups which prevents from easily hydrolysing and gain good alignment on film surface after curing. Moreover, the umbrella-like structure of the $Si(OSi(CH_3)_3)_3$ functional groups confers low surface energy to the treated fabrics allowing them to not only repel water but also fatty acid triglycerides like olive oil, as well as heavy oils (motor oil or mineral oil). These authors demonstrated that M3T-containing (co)polymethacrylates can provide omniphobic surfaces with good anti-stain properties when white spirit is used as solvent for the coating procedure, being the performance of the product reduced when using other organic solvents. However, no studies have been found regarding the synthesis and textile application of waterborne emulsions of M3T and bio-based methacrylic copolymers. As most silicon-containing acrylates, M3T is a prohibitively expensive material. Thus, M3T copolymerization with bio-based acrylates could be an interesting option to reduce price and at the same time investigate synergies while increasing sustainability. As it is well known, the most ideal solvent for chemical reactions is water, which is green and nontoxic. Academic and industrial areas have a strong desire for waterborne coatings. However, water is rarely used as a carrier for low surface tension chemicals because of the poor dispersibility of these materials which makes it very difficult to obtain stable emulsions or dispersions [36-38].

This paper reports the synthesis of a series of waterborne fluorine-free M3T-containing (co)polymethacrylates with remarkable water and oil repellence (WOR) properties. The (co)polymers were obtained by emulsion polymerization using stearyl methacrylate (SMA), a methacrylic comonomer with high bio-content. The conversion degree of the (co)monomers has been qualitatively verified by Fourier-transform infrared spectroscopy (FTIR). Structure and properties of the obtained (co)polymers has been assessed by nuclear magnetic resonance (NMR), differential scanning calorimetry (DSC), thermogravimetric analysis (TGA) and energy-dispersive X-ray spectroscopy (EDS). Moreover, the particle size, particle size distribution and stability of the developed emulsions have been tested by laser diffraction spectrometry (LDS) and Z-potential measurements. Afterwards, the M3T-containing copolymethacrylates were applied onto a hydrophilic cotton fabric by padding method at several product dosages and the textile surface and WOR performance was then characterized by scanning electron microscopy (SEM), EDS element mapping, X-ray fluorescence (XRF) and contact angle measurements with water and olive oil. Results were evaluated against conventional C6 fluorinated textiles. The effect of M3T content in the copolymer and the copolymer dosage in the padding liquor have been studied and related to the textile's WOR performance. Based on the obtained results, the application of the new coated textiles for anti-stain finishing and solvent separation processes have been proposed and demonstrated.

2. Experimental

2.1. Materials

3-[Tris(trimethylsilyloxy)silyl]propyl methacrylate (M3T) is a silicone-based methacrylate with a molecular weight of 422.8 g/mol and it has been supplied by Wacker Chemie AG. Fatty alcohol methacrylic ester Visiomer Terra C17,4-MA (SMA) is a methacrylic compound with a bio-content of 81% (calculated as ratio of C-number alcohol to C-number methacrylate) and an average molecular weight of 330 g/mol, it has been purchased from Evonik Industries AG. Chemical structures of the two monomers are shown in Figure 2. Isotridecyl alcohol ethoxylated (IAEO) with HLB=16.5, required to obtain stable emulsions of these monomers, was purchased from BASF (Lutensol TO 20, isotridecyl alcohol condensed with 20 moles of ethylene oxide). 2,2'-Azobis(2-methylpropionamidine)dihydrochloride (V-50) was supplied by Fujifilm. All the chemicals were used without further purification. CENTERGARD C6 PS is a C6 fluorocarbon commercialised by COLOR CENTER, S.A.; it is a waterborne fluorocarbon with an active content around 29% and it is widely employed in the textile finishing sector as a high-performance fluorinated WOR agent for technical textiles.

Cotton fabric, desized, alkaline scoured and peroxide pre-bleached to remove all the impurities was supplied by INOTEX spol. s r.o. and was used as a substrate to perform the coatings without further (pre)treatment. The main characteristics of the cotton fabric are summarized as follows: composition 100% cotton; width (EN 1773) 150 cm; set (threads/cm, EN 1049-2) warp = 53.5 / weft = 28.5; weave twill 280; yard count (ISO 1144) warp/weft: 20 tex, cotton ring spun-combed; square weight = 158 g/m^2.

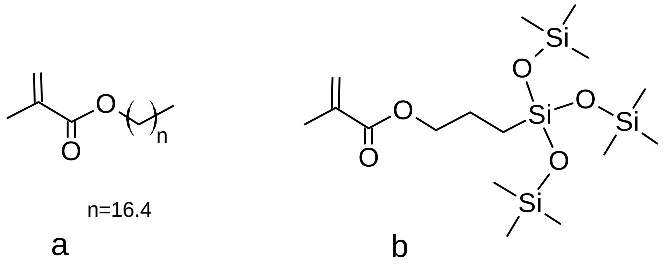

Figure 2. Chemical structure of: a) SMA and b) M3T monomers

2.2. Synthesis of M3T based copolymers and emulsions

(Co)polymers of M3T and SMA were synthesized by emulsion polymerization using the water-soluble azo initiator V-50. A typical process for the emulsion polymerization of the two components copolymer is described as follows: 21.0 g (50 mmol) M3T, 16.8 g of SMA (50 mmol), V-50 0.25 g (0.66% weight ratio based on total monomer), 3.8 g of IAEO (10.0% weight ratio based on total monomer) and 88.5 ml of deionized water were charged into a 250 mL three-neck round bottom flask equipped with a reflux condenser. The mixture was heated to 40 ºC and stirred with mechanical impeller at 1500 rpm for 15 min.

Afterwards the mixture was ultrasonicated until a homogeneous Tindall emulsion was achieved, then the monomer emulsion was degassed with nitrogen using two vacuum/N_2 cycles. The temperature of the mixture was raised to 65 ºC and held for 6 h at 500 rpm under nitrogen blanketing to ensure complete monomer conversion. The obtained waterborne (co)polymer emulsions, with a polymer content of 29%, are summarized in Table 1 and were used without further purification to perform all the application tests on textile fabrics. On the other hand, a small amount of each waterborne emulsion was purified for chemical characterization purposes. The following purification procedure was followed: a small amount of the obtained polymer emulsion was precipitated by adding ethanol and washed several times with ethanol/acetone 50/50 v/v to wash-off the emulsifying system, then the obtained pure (co)polymer was dried in an oven at 60 ºC for 24 h to completely remove traces of water and solvents.

Table 1. Series of methacrylic copolymers obtained from fluorine-free hydrophobic monomers

Sample	Amount of M3T (molar %)	Amount of SMA (molar %)
PM3T	100	0
$PM3T_{75}SMA_{25}$	75	25
$PM3T_{50}SMA_{50}$	50	50
$PM3T_{25}SMA_{75}$	25	75
PSMA	0	100

2.3. Application of M3T based copolymers on cotton fabrics

As a substrate, a highly hydrophilic woven cotton fabric, previously bleached and cleaned to remove impurities, has been employed. The cotton fabric is immersed in the bath liquor containing the WOR finishing agent (original copolymer emulsion diluted with deionized water at the indicated dosage), the excess of liquor absorbed by the fabric is removed by squeezing between two rotating rollers at controlled pressure and speed (Foulard Mathis operating at a pressure of 2 bar), the measured average wet pick-up of the impregnated fabrics was within 65 and 67%. Finally, the impregnated fabric at the exit of the foulard is placed horizontally in a drying oven (Mathis Labcoater), at a drying temperature of 120 ºC for 2 minutes, with a subsequent curing step at 160 ºC for 1 minute. As a reference, cotton fabrics have been also coated with C6 fluorocarbon CENTERGARD C6 PS.

2.4. Characterization techniques

2.4.1. Characterization of synthesized copolymers and emulsions

A small amount of each waterborne emulsion was precipitated to isolate the polymer which was further purified for subsequent chemical characterization. Fourier transform infrared spectroscopy (FTIR) was employed to qualitatively assess monomer conversion during polymerization. FTIR spectra were obtained using a Perkin Elmer Spectrum Two infrared equipment equipped with an ATR accessory. Forty scans were taken for each sample with a resolution of 8 cm^{-1}. A small portion of the reaction sample was previously treated at mild temperature under IR lamp to evaporate water, before performing FTIR spectra. Structural characterization of (co)polymers was performed by nuclear magnetic resonance (^1H NMR and ^{13}C NMR), using a Bruker AMX-300 spectrometer at 25.0 °C operating at 300.1 and 75.5 MHz, respectively. Samples were dissolved in deuterated chloroform, and spectra were internally referenced to tetramethylsilane (TMS). About 10 and 50 mg of sample dissolved in 1 mL of solvent were used for ^{1}H and ^{13}C NMR, respectively. Sixty-four scans were acquired for ^{1}H and 1000−10 000 for ^{13}C with 32K and 64K data points as well as relaxation delays of 1 and 2 s, respectively. Molecular weight analysis was performed by gel permeation chromatography (GPC) on a Waters equipment provided with RI and UV detectors. 100 µL of 0.1% (w/v) sample solution was injected and chromatographed with a flow of 0.5 mL/min using as solvent THF. PL1110-1520 and PL1110-6500 Agilent linear PLgel columns (7.5 mm×300 mm, pore size 10^3–10^4 Å) packed with cross-linked polystyrene and protected with a precolumn were used. Molecular weight averages and distributions were calculated against PMMA standards. Differential scanning calorimetry (DSC) studies of the obtained (co)polymers have been carried out to determine their melting temperature (T_m), crystallization temperature (T_c), melting enthalpy (ΔH_m) and crystallization enthalpy (ΔH_c) as well as possible second-order transitions such as glass transition temperature. Samples were heated from -70 to 150 ºC at a constant heating rate of 10 ºC/min in a Perkin Elmer model Pyris I under nitrogen atmosphere (50 mL/min), working with 5 mg samples placed in sealed aluminium pans. Second order transitions (T_g) were determined by the StepScan DSC technique that yields enhanced characterization information by separating out the reversible and irreversible thermal events. Measurements were run from -100 ºC to 100 ºC at a heating and cooling rates of 4 and 2 °C/min respectively, a modulation of amplitude of 1 °C and a period of 60 s. The thermal stability of the synthetized (co)polymers have been studied by thermogravimetric analysis (TGA) under nitrogen and oxidative conditions, using a Mettler Toledo TGA2 equipment. The thermogravimetric analysis consisted of recording the weight loss of the samples subjected to a temperature gradient from 25 ºC to 600 ºC at 10 ºC/min in a furnace with nitrogen or air atmospheres. Finally, the elemental composition of the copolymers has been analysed by Energy-Dispersive X-ray Spectroscopy (EDS), depositing a drop of each emulsion on a silicon wafer.

Moreover, the particle size and the particle size distribution (PSD) of developed aqueous polymeric emulsions have been characterized by Laser Diffraction Spectrometry (LDS). PSD is usually determined over a list of particle size ranges that covers nearly all sizes present in the sample. Polymer dispersity index (PdI) is used to evaluate the dispersion of PSD. LDS measurements were done in a Malvern Mastersizer 2000 instrument (Worcestershire, UK), using water as the dispersion media. A particle Refractive Index of 1.55 was considered for the analysis and 3 measurements were done for each sample. The stability of the dispersions was determined by Z-potential measurements using a Malvern Zetasizer ZS equipment.

2.4.2. Characterization of coated textiles

The surface morphologies of the cotton fibres were observed by scanning electron microscopy (SEM) using an Ultra Gemini-II microscope from Carl Zeiss SMT, also equipped with Energy-Dispersive X-ray Spectroscopy (EDS) which has been employed for element mapping analysis on textile surface. Moreover, X-ray Fluorescence (XRF) was used to perform a semi-quantitative measurement of certain elements on the surface of the treated fabrics using a Bruker S8 TIGER wavelength dispersive X-ray fluorescence spectrometer using vacuum for the analysis.

Water and oil-repellence of the treated cotton fabrics has been tested by a goniometer (SURFTENS Universal) by measuring the contact angle (θ) of a droplet of water (WCA) and olive oil (OCA) placed on the surface of the coated textile. The volume of each liquid droplet was 5 μL and the average value of five measurements, made at different positions of the textile surface, was adopted as the value of WCA or OCA. The sliding angle was measured by manually tilting the stage table of the goniometer. Finally, surface free energies of the copolymethacrylates were determined according to the method by Owens and Wendt [39].

Anti-stain performance of the cotton fabrics treated with the (co)polymer emulsions at a dosage of 60 g/L has been evaluated. Five low viscosity liquids were chosen (water, coffee, red wine, juice+milk, olive oil). The surface tension of these liquids is shown in Table 2.

Table 2. Surface tension of liquids employed for anti-stain test (literature values for 20-25ºC)

Liquid	**Surface tension (mN/m)**
Water [2]	71.4 - 72.9
Juice [40]+milk [41]	52.0 – 54.0
coffee [42]	46.2 - 48.7
red wine [43]	43.6 - 47.6
olive oil [1]	32.0 - 33.1

The treated fabrics were first allowed to rest for 48 h and 60% relative humidity, then 50 μL drops of each liquid were carefully placed on the substrate's surface via a pipette. The staining agents were allowed to remain on the surface for 5 min, afterwards the remaining drops were removed carefully by absorbent towel and the anti-stain performance was evaluated by 5 level ratings (Table 3).

Table 3. Anti-stain performance rating scale

Rating number	**Appearance of the textiles**
4	drop remains on the fabric's surface after 5 min., no wetting is observed, no stain residue remains after removing the drop
3	drop remains on the fabric's surface after 5 min., no wetting is observed, slight stain residue remains after removing the drop
2	partial wetting of the fabric surface by the drop after 5 min., stain residue remains after removing the drop
1	partial wetting of the fabric surface by the drop after 5 min., clear visible stain residue remains after removing the drop
0	complete wetting of the fabric surface by the drop after 5 min

Air permeability, tensile strength and elongation of the treated and untreated fabrics have been tested. Air permeability was tested using a POLYMERTEST (Zlín, CR) using a pressure difference of 200 Pa and a sample area of 20 cm^2 according to EN ISO 9237. Tensile strength and elongation were tested using the strip method in a SDL M350-10kN (TESTOMETRIC ROCHDALE, England), with a test speed of 100 mm/min according to EN ISO 13934-1.

The solvent-water separation efficiency of the fabrics coated with all the finishing agents at a dose of 60 g/L was measured by a filtration process of a mixture of water and a solvent which is immiscible with water. Water has a high surface tension (72.86 mN/m at 25 °C) while the selected solvent, chloroform, has a surface tension as low as 26.67 mN/m at 25 °C. A mixture containing 25 g of chloroform and 25 g of water was employed to investigate the separation efficiency of the hydrophobic fabrics. The mixture was slowly poured into the filtering equipment (see Figure 12) where there is already placed the fabric. The hydrophobic fabric was reused 10 times. In each test, the amount of chloroform is adjusted as it evaporates during the process. The mass of water recovered in each filtration cycle has been recorded. Moreover, the treated fabrics were also employed for solvent-water separation employing a mixture of n-hexadecane (surface tension of 27.30 mN/m at 25 °C) and water. A different test configuration has been employed as n-hexadecane is a light oil which floats on top of the water. The fabrics were employed to prepare a bag in which pristine polyurethane (PU) sponges were filled to achieve high oil absorption capacity. A mixture containing 20 g of n-hexadecane and 60 g of water was employed. The weight of water was measured after the separation cycle.

3. Results and discussion

3.1. Characterization of the synthetized polymeric emulsions

(Co)polymers of M3T and SMA were synthesized by emulsion polymerization using water as a polymerization media. Monomer conversion during polymerization was qualitatively assessed by ATR-FTIR spectroscopy in the MIR region. Figure 3 shows the FTIR spectra of $PM3T_{50}SMA_{50}$ for the initial monomer emulsion of and after polymerization for 6h at 65 ºC. The peaks that clearly disappear during polymerization are: 1639 cm^{-1} (C=C stretching), 935 cm^{-1} (out of plane bending of C-H from the double bond). Also the peaks at 1320 and 1294 cm^{-1} assigned to asymmetric and symmetric stretching vibrations of the C-O bond from the ester groups of methacrylate monomers disappear, shifting to lower frequencies, once the monomers are polymerized. The disappearance of the peak at 1639 cm^{-1} has been specifically taken as a reference for qualitative assessment of monomer conversion. Similar spectra were obtained after polymerization of all the (co)polymers. FTIR spectra of monomers, emulsifier and catalyst employed in the synthesis has been also recorded and reported in Supplementary Information (Figures S1 and S2).

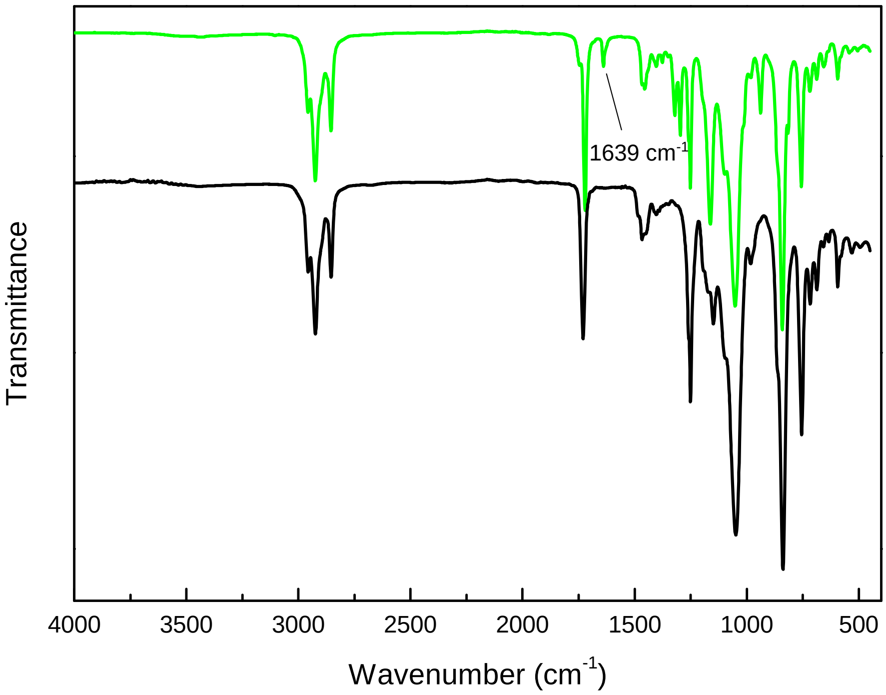

Figure 3. FTIR spectra in the MIR region for PM3T$_{50}$SMA$_{50}$ sample before (top, green) and after polymerization (bottom, black)

^{1}H and ^{13}C NMR spectra of all PM3T$_x$SMA$_y$ copolymers were recorded, thus confirming chemical structure, tacticity and (co)polymer composition. ^{1}H and ^{13}C NMR spectra of PM3T$_{50}$SMA$_{50}$ with peak assignments are depicted in

Figure *4*. Full spectral width ^{1}H NMR spectrum is depicted in Figure S3. Spectra of all the series are included in the Supplementary Information (Figure S4 and S5, for ^{1}H NMR and ^{13}C NMR, respectively). Copolymer composition was determined by integration of signals corresponding to the Si-CH$_3$ and Si-CH$_2$ protons of M3T units appearing at 0.1 and 0.4 ppm respectively (peaks 8 and 7) and the signals due to the rest of the protons of both M3T and SMA units (Figure S3). A good correlation between M3T/SMA feed molar ratio and the determined by ^{1}H NMR was observed, indicating that both monomers were fully incorporated in the final copolymer (Table 4). On the other hand, ^{13}C NMR signals due to main chain carbons were used to determine the tacticity of the (co)polymers. These signals were observed to split into different peaks due to stereoregularity effects (Figure 5). As an example, each of the signals due to CH$_3$ and C carbons were observed to split into two broad peaks corresponding to syndiotactic (rr) and heterotactic (mr/rm) triads. Signals due to isotactic (mm) triads were almost not detected because these copolymers were observed to be predominantly syndiotactic. By integration of these peaks the degree of syndiotacticity was determined, which was around 80% for all (co)polymers studied (Table 4).

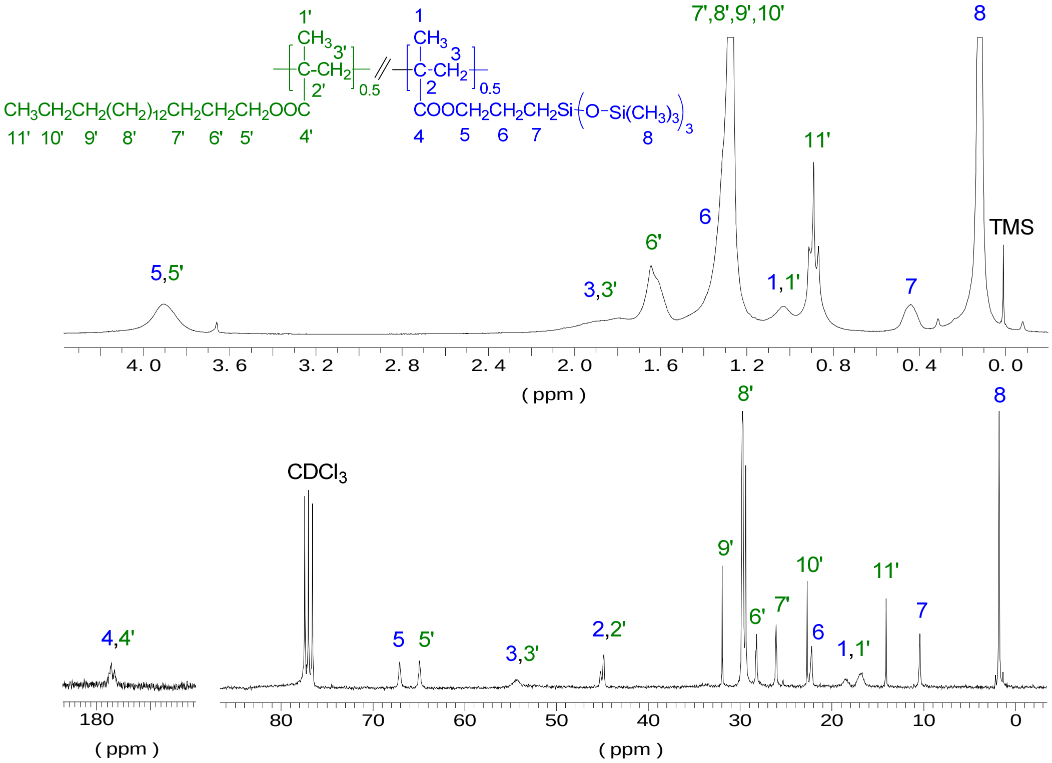

Figure 4. ^{1}H NMR (top) and ^{13}C NMR (bottom) spectra of PM3T$_{50}$SMA$_{50}$ with peak assignments

Copolymers of high molecular weights were achieved with M_n values between 244,000 and 425,400 and dispersities between 1.3-1.6 (Table 4).

Table 4. Molecular weights, composition and tacticity of PM3T, PSMA and M3T-containing copolymethacrylates

Polymer	**Feed composition**[a] **[M3T]/[SMA]**	**Copolymer Composition**[b] **[M3T]/[SMA]**	**Tacticity**[c] **m/r**	M_n[d]	Đ[d]
PM3T	100/0	100/0	16.6/83.4	248,100	1.4
PM3T$_{75}$SMA$_{25}$	75/25	73.8/26.3	17.1/82.9	326,750	1.5
PM3T$_{50}$SMA$_{50}$	50/50	49.2/50.8	18.4/81.6	295,960	1.6
PM3T$_{25}$SMA$_{75}$	25/75	27.0/73.0	19.9/80.1	244,564	1.3
PSMA	0/100	0/100	17.1/82.9	425,389	1.5

[a] Molar ratio in the initial feed.

[b] Molar ratio in the (co)polymer determined from ^{1}H NMR spectra.

[c] Tacticity determined by integration and averaging of CH_3 (1,1’ peaks) and C (2,2’ peaks) which are sensitive to stereoregularity (m: meso or isotactic dyads and r: racemic or syndiotactic dyads).

[d] Number average molecular weights (M_n) and dispersities (Đ) determined by GPC.

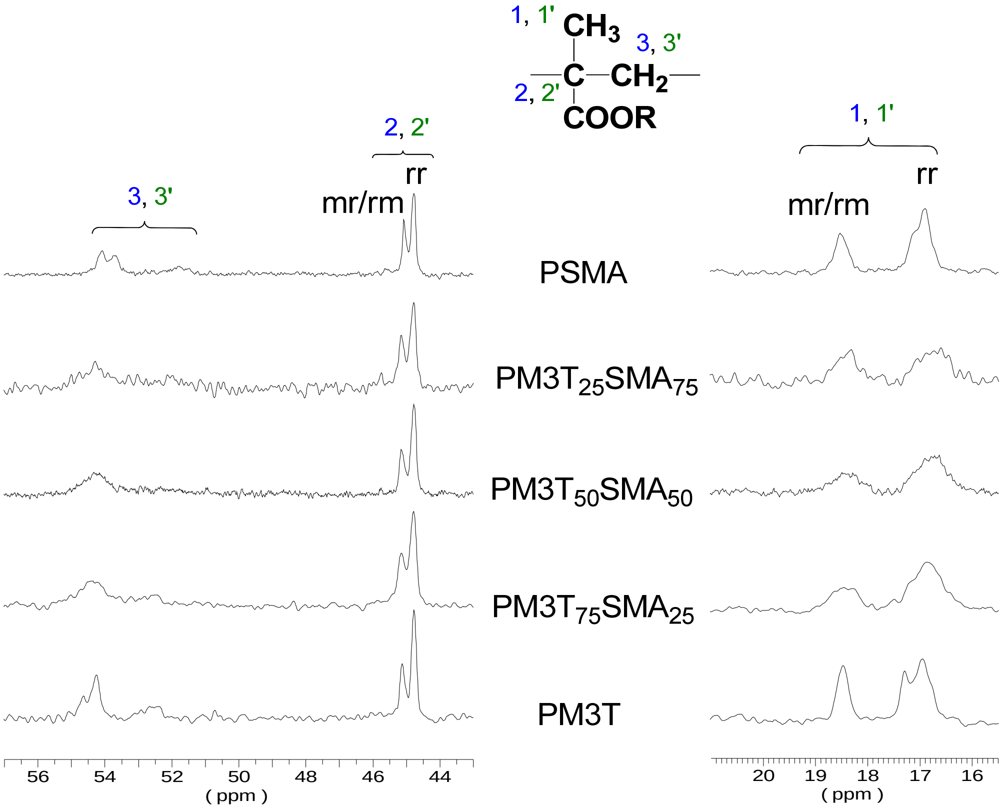

Figure 5. Expanded ^{13}C NMR spectra of PM3T, PSMA and M3T-containing copolymethacrylates in the region of the main chain CH_2 (3,3'), C (2,2') and CH_3 (1,1') carbons with peak assignments to different stereosequences

The thermal properties of the developed (co)polymers have been analysed by DSC and TGA. The non-isothermal DSC thermograms for PM3T, M3T-containing copolymethacrylates and PSMA are shown in Figure 6. The crystallization and melting temperatures and enthalpies and glass transition temperatures taken from these thermograms are shown in Table 5. The DSC thermogram of PSMA displayed a clear melting peak at 32.6 ºC, and a crystallization peak at 19.9 ºC, with fusion and crystallization enthalpies of 50.0 and 45.4 J/g, respectively, indicating its crystalline nature and attributed to lamellar packing of paraffinic side chains. The glass transition temperature (T_g) of PSMA has not been observed, not by DSC, not by StepScan DSC, that could be associated to a low content of amorphous phase on this polymer. On the other hand, the homopolymer PM3T only showed a second order transition at 2.0 ºC, shown in Supplementary Information (Figure S6), ascribed to the T_g of the sample, which indicates the completely amorphous structure of the material. This can be assigned to the bulkiness of the M3T side groups that doesn't allow them to arrange in a crystalline structure. DSC thermograms of copolymers with SMA content ≥ 50 molar% ($PM3T_{50}SMA_{50}$ and $PM3T_{25}SMA_{75}$) showed the presence of a melting and a crystallization peak, their enthalpies decreasing, and their melting and crystallization temperatures shifting to lower values as M3T content increases, suggesting that both comonomers are randomly incorporated in the chain during the emulsion polymerization. On the other hand, $PM3T_{75}SMA_{25}$ does not show first order transitions and a second order transition at -31 ºC (Figure S6) due to T_g was observed for this copolymer. The incorporation of the M3T comonomer at random into the polymer chain restricts the packing of the paraffinic side chains reducing the observed melting temperature or preventing its crystallization.

The thermal stability of the synthetized (co)polymers with temperature has been studied by TGA and curves are collected in Figure S7. The degradation temperatures corresponding to a weight loss of 10% and the temperatures of the maximum degradation rate are collected in Table 5. All the (co)polymers have sufficient thermal stability to withstand without degradation the temperature conditions that are required to be applied on the fabrics (drying at 120 ºC followed by curing at 160 ºC for 1 minute).

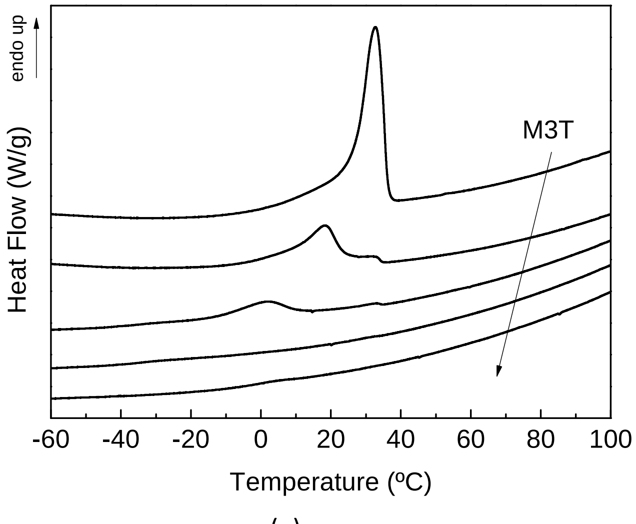

(a)

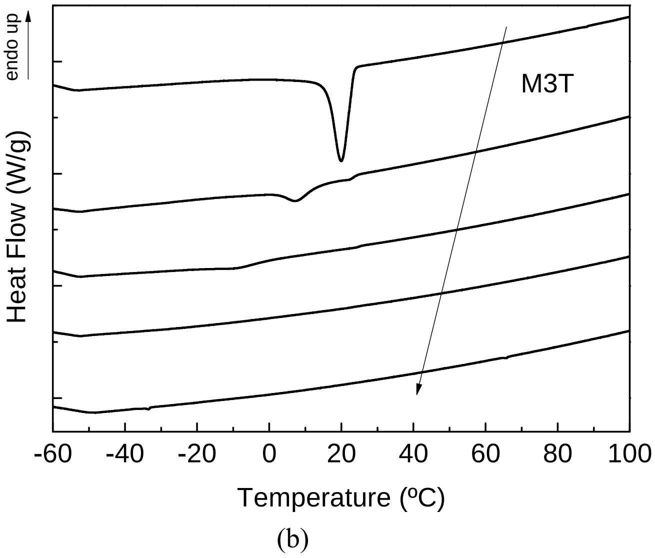

(b)

Figure 6. Second heating (a) and cooling (b) DSC thermograms of the methacrylic (co)polymer. From top to bottom PSMA, $PM3T_{25}SMA_{75}$, $PM3T_{50}SMA_{50}$, $PM3T_{75}SMA_{25}$, PM3T.

!

Table 5. Thermal properties of PM3T, PSMA and M3T-containing copolymethacrylates!

Polymer	**DSC Second Heating**[b]			**DSC Cooling**[b]		**TGA (N$_2$)**		**(Air)**	
	T_g[a] (ºC)	**T_m (ºC)**	**ΔH_m (J/g)**	**T_c (ºC)**	**ΔH_c (J/g)**	**^oT_d[c] (ºC)**	**T_d[d] (ºC)**	**^oT_d[c] (ºC)**	**T_d[d] (ºC)**
PM3T	2.0	-	-	-	-	286.5	343.3	260.8	287.0
PM3T$_{75}$SMA$_{25}$	-31.0	-	-	-	-	266.6	323.5	246.2	299.1
PM3T$_{50}$SMA$_{50}$	-	2.5	5.5	-9.0	6.5	276.2	340.9	254.8	295.2
PM3T$_{25}$SMA$_{75}$	-	18.5	23.5	7.5	28.0	299.6	341.5	257.6	312.3
PSMA	-	32.5	50.0	20.0	45.5	278.5	325.5	266.6	332.2

[a] Glass-transition temperature taken as the inflection point of the heating step scan DSC.

[b] Melting (T_m) and crystallization (T_c) temperatures and their respective enthalpies (ΔH_m, ΔH_c) measured by DSC at heating / cooling rates of 10ºC min $^{-1}$.

[c] Temperature at which a 10% weight loss was observed in the TGA traces recorded at 10 ºC min $^{-1}$.

[d] Temperature of maximum degradation rate.

The qualitative elemental composition for the synthetized polymethacrylates and reference C6 fluorocarbon, obtained by EDS, is shown in Table 6. A drop of each concentrated emulsion has been analysed. EDS values, although they are semiquantitative, show a good correlation with the expected values from the theoretical ratio of monomers in the feed during the synthesis. As it is expected, silicon content determined by EDS decreases as the molar content in M3T in the copolymer decreases. All the samples in the PM3T$_x$SMA$_y$ series are fluorine-free, therefore showing no detectable fluorine. By contrast, fluorocarbon CENTERGARD C6 PS presents a high elemental fluorine content and also some chlorine content arising from the C6-perfluorinated methacrylate and vinylidene chloride monomers, respectively, both employed in the synthesis.

Table 6. Elemental analysis (wt.%) carried out by EDS for PM3T, M3T-containing copolymethacrylates and reference C6 fluorocarbon

Element	**PM3T**	**PM3T$_{75}$SMA$_{25}$**	**PM3T$_{50}$SMA$_{50}$**	**PM3T$_{25}$SMA$_{75}$**	**PSMA**	**C6_PS**
C	52.8	57.8	65.5	77.3	85.0	43.1
O	22.9	21.7	19.3	14.5	14.1	8.2
Si	24.3	20.5	15.2	8.2		
F						41.0
Cl						7.7

Finally, the emulsion stability, the particle size and particle size distribution of emulsions derived from M3T-containing copolymethacrylates have been investigated. Particle size distribution (PSD) curves of all developed aqueous polymeric emulsions analysed by LDS are shown in Figure S8 and particle size and PdI values are summarized in Table 7. As an example, Figure 7 collects the particle size distribution curve of PM3T$_{50}$SMA$_{50}$ copolymer and C6 PS product. It is found that particle size distribution curves are unimodal for PM3T, PSMA and all M3T-containing copolymethacrylates, whereas C6 fluorocarbon product presented some agglomerates at higher particle sizes. The average particle sizes (d$_{50}$) were around 180 nm for all the emulsions in the PM3T$_x$SMA$_y$ series and polymer dispersity indexes (PdI) are close to 0.1, indicating that products had satisfactory stability and good dispersibility. The smaller the value of PdI, the better the homogeneity of emulsion [44].

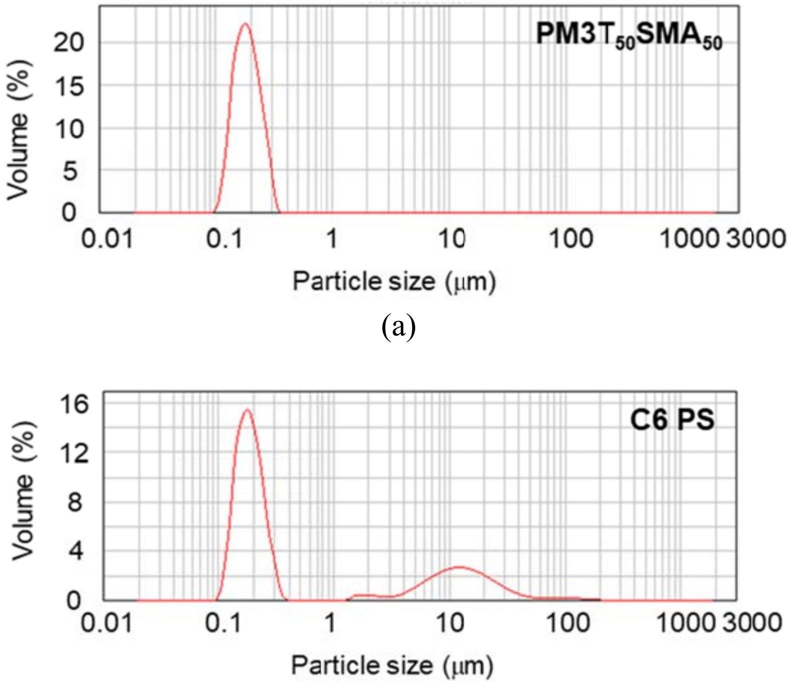

(a)

(b)

Figure 7. Particle size distribution obtained by LDS for: a) PM3T$_{50}$SMA$_{50}$ and b) reference C6 fluorocarbon

Table 7. Particle size PdI and Z-potential obtained by LDS for PM3T, PSMA, M3T-containing copolymethacrylates and reference C6 fluorocarbon

	d(10) (nm)	d(50) (nm)	d(90) (nm)	PdI	Z potential (mV)
PM3T	133	180	252	0.102	+ 33
PM3T$_{75}$SMA$_{25}$	134	182	256	0.104	+ 41
PM3T$_{50}$SMA$_{50}$	139	192	288	0.111	+ 48
PM3T$_{25}$SMA$_{75}$	137	177	224	0.114	+ 43
PSMA	128	162	194	0.132	+ 41
C6_PS	139	212	363	0.357	+ 33

The stability of the dispersions was determined by Z-potential. Measurements have been carried out diluting samples at 40 g/L with sample matrix solution. The Z potential curves of the samples are shown in Supplementary Information (Figure S9) and Z potential values are collected in Table 7. As expected, the zeta potential of C6 fluorocarbon product is higher than +30 mV, indicating their good stability and adhesion to anionic substrates [44-45]. For all the PM3T$_x$SMA$_y$ series, the zeta potential presented similar or even higher positive values indicating their high stability. These positive values could be ascribed to the ammonium chain ends produced by the initiating species which are supposed to be placed in the shell of the micelles.

3.2. Characterization of textiles coated with the PM3T$_x$SMA$_y$ emulsions

To test the performance of synthetized emulsions as WOR finishing agents for textiles, they have been applied on cotton fabrics by padding. SEM micrographs of untreated and treated cotton with PM3T$_x$SMA$_y$ emulsions are illustrated in Figure 8. The untreated cotton fibres showed smooth surface and cylindrical structures with diameters between 5-20 µm. After the cotton fabric was coated by PM3T and PM3T$_{75}$SMA$_{25}$ at a dose of 60 g/L, an evidently roughness was generated on the surface. However, when the SMA_content is increased in the copolymers it was observed that the coating became more smooth. Good film-forming properties were observed from SEM images for all the (co)polymers, similar to the film-forming properties of C6 fluorocarbon. Moreover, three dosages of PM3T and PM3T$_{75}$SMA$_{25}$ finishing agent have been applied on cotton fibres. SEM images, collected in Figure 9, showed that a dose of 100 g/L is too high as the fibers begin to stick together.

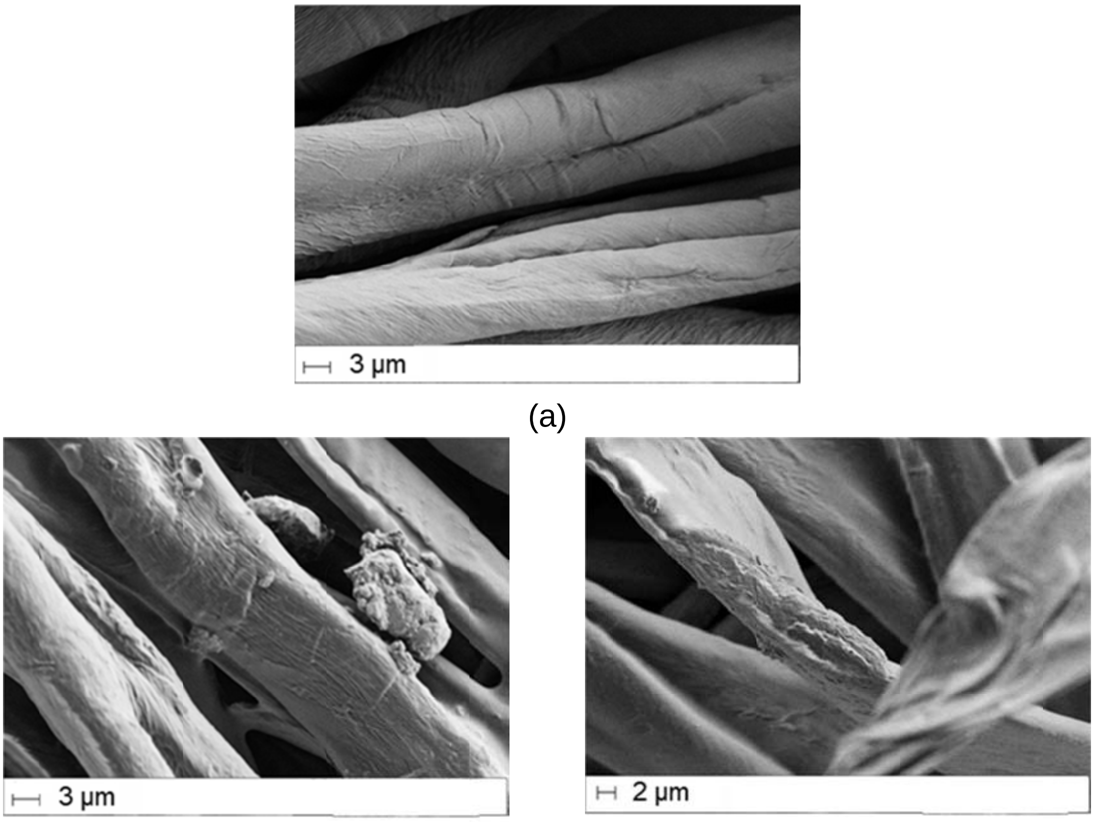

(a)

(b)

(c)

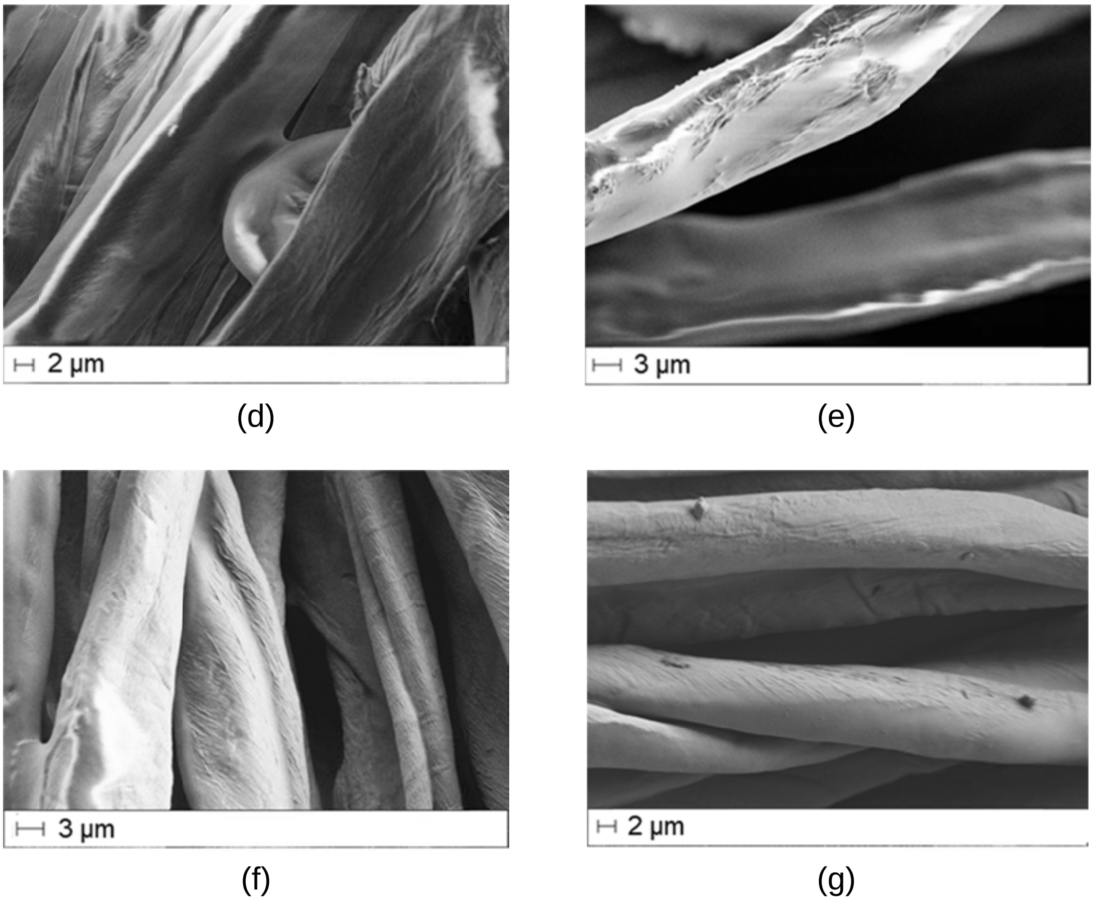

Figure 8. SEM micrographs for: (a) untreated cotton and coated cotton fabrics: (b) PM3T, (c) PM3T$_{75}$SMA$_{25}$, (d) PM3T$_{50}$SMA$_{50}$, (e) PM3T$_{25}$SMA$_{75}$, (f) PSMA and (g) C6 PS with a dosage of 60 g/L. Micrographs have been obtained with a magnification of x2000 and 3.3 mm of working distance

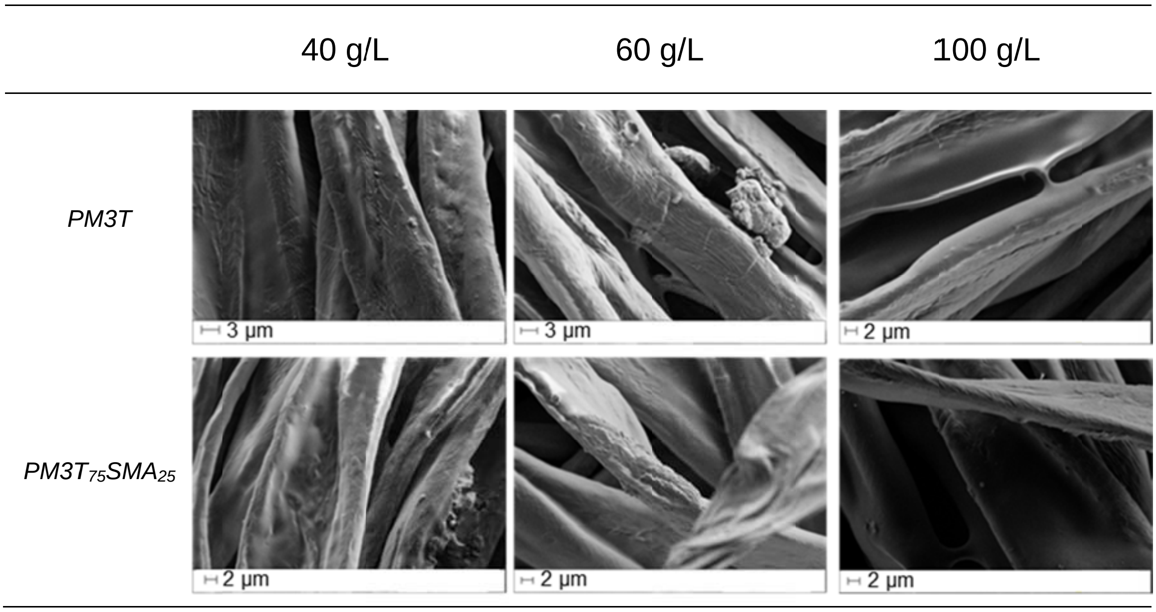

Figure 9. SEM micrographs for PM3T and PM3T$_{75}$SMA$_{25}$ coated cotton textiles with a dosage of 40, 60 and 100 g/L. Micrographs have been obtained with a magnification of x2000 and 3.3 mm of working distance

The homogeneous distribution of the product on the cotton fabric has been assessed by EDS mapping analysis of elemental silicon, fluorine and chlorine, as can be seen in Figure 10.

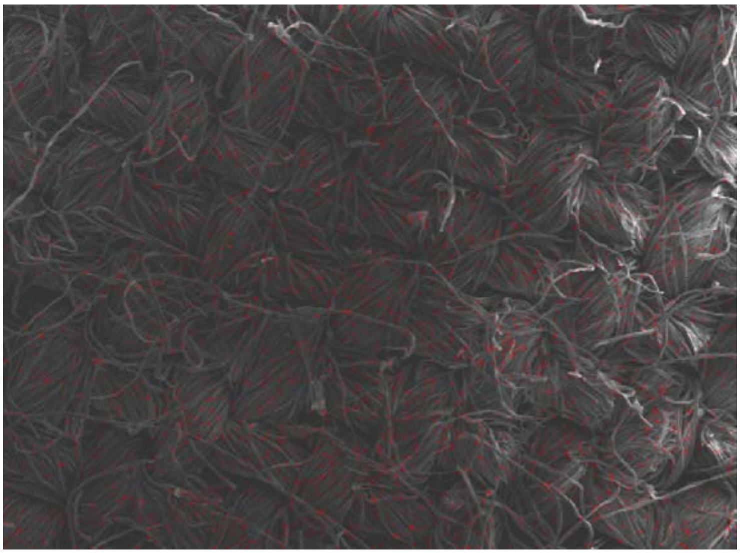

(a)

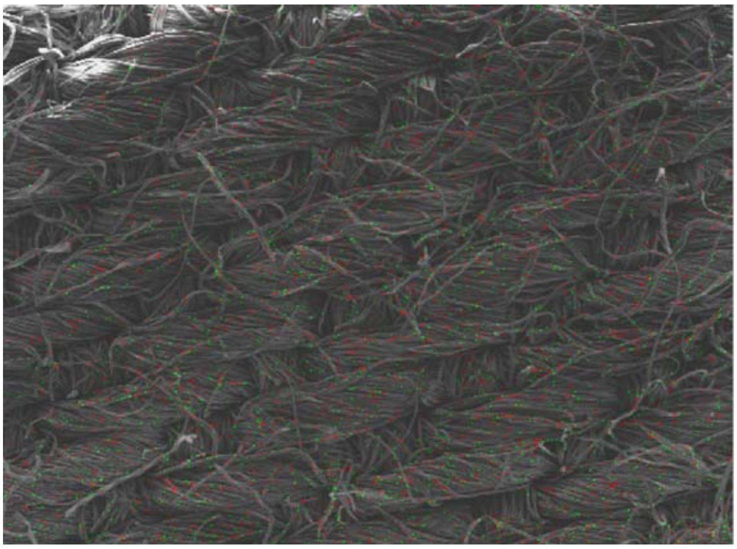

(b)

Figure 10. EDS mapping of coated cotton textiles with doses of 60 g/L of: a) PM3T$_{75}$SMA$_{25}$ emulsion (silicon in red) and b) C6 PS fluorocarbon (fluorine in green and chlorine in red)

To quantitatively characterize the distribution of elements of interest like Si and F on the fabrics' surface, XRF technique has been applied, obtaining consistent results. Table 8 shows the elemental analysis of the cotton fabrics coated with the (co)polymethacrylate series. The analysis of the different fabrics applied with 60 g/L of the corresponding finishing agent showed a decreasing content of silicon with the decrease in M3T content in the (co)polymer. In addition, silicon content is in a good agreement with EDS analysis. Some other elements such as Ca, S and Fe were also detected in similar amounts on all the fabrics (treated and untreated), indicating that these elements were present on the fibre as impurities. Chlorine, however, comes from the radical initiators used in the synthesis process. XRF analysis of C6 fluoropolymers showed also a high content of fluorine and chlorine elements on the samples. Differences in the element content between EDS and XRF can be ascribed to the fact that EDS directly analyses the polymers while XRF analyses the surface of the coated fabrics. The different measuring depth of X ray of both techniques could also contribute to this difference. When different doses of PM3T and $PM3T_{75}SMA_{25}$ finishing agents have been applied on cotton fibres, the amount of silicone on the surface increased proportionally.

Table 8. Atomic concentration (%) by XRF for untreated and coated cotton textiles

Product applied on cotton fabric (dosage)	XRF (%)					
	Si	Cl	Ca	S	Fe	F
Untreated cotton	0.01	0.04	0.22	0.01	0.02	-
PM3T (40 g/L)	0.87	0.07	0.20	0.03	0.04	-
PM3T (60 g/L)	1.43	0.08	0.21	0.04	0.03	-
PM3T (100 g/L)	2.27	0.07	0.21	0.03	0.03	-
$PM3T_{75}SMA_{25}$ (40 g/L)	0.81	0.07	0.21	0.03	0.02	-
$PM3T_{75}SMA_{25}$ (60 g/L)	1.11	0.07	0.21	0.03	0.06	-
$PM3T_{75}SMA_{25}$ (100 g/L)	1.67	0.08	0.20	0.03	0.04	-
$PM3T_{50}SMA_{50}$ (60 g/L)	0.74	0.08	0.21	0.03	0.08	-
$PM3T_{25}SMA_{75}$ (60 g/L)	0.39	0.08	0.23	0.03	0.09	-
PSMA (60 g/L)	0.01	0.09	0.25	0.03	0.04	
C6 PS (60 g/L)	0.02	0.79	0.22	0.05	0.03	0.91

Water and oil-repellence of the textile surfaces has been characterized by using de-ionized water and olive oil to determine the surface wettability of coatings. Table 9 lists the values of the static water and oil contact angles and the tilt angles, obtained for all samples with the different product doses and the time that a droplet of water and olive oil remained on surface for the fabrics impregnated with the WOR agents at a dose of 60 g/L. It is well known that untreated cotton quickly absorbs water and olive oil and therefore, droplets do not remain on the surface time enough to measure the contact angle. When the cotton fabric was coated by M3T-containing (co)polymethacrylates, these values were dramatically improved and revealed a good repellence towards water and olive oil, at some extent.

Figure *11* shows the images of the water and oil drops on cotton textile coated with $PM3T_{75}SMA_{25}$ as an example. WCA are quite stable with SMA content and remain on surface more than 3600 s with an angle around 127-133º. OCA increases slightly as the SMA content increases to certain extent, going from 110º for 0% SMA, reaching a plateau for SMA content between 25 and 50% and decreasing again for SMA content ≥75%. WCA and OCA are also similar to those obtained with the C6 fluoropolymer at this initial time. The similarity of all the values indicates a great contribution of the surface texture/porosity of the fabric [1]. The roughness generated on the surface of these cotton fabrics by the coating, shown in Figure 8, could contribute to this behaviour.

Table 9. Values of water and olive oil static contact angles and water and olive oil tilt angles for untreated and coated cotton textiles

Product applied on cotton fabric (dose)	Water static contact angle (θs) (º)	Time that the water's droplet remains (s)	Tilt angle for water (º)	Olive oil static contact angle (º)	Time that the olive oil's droplet remains (s)	Tilt angle for olive oil (º)
Untreated cotton	absorbed	absorbed	absorbed	absorbed	absorbed	absorbed
PM3T (40 g/L)	119 ± 1	-	30 ± 3	101 ± 1	-	49 ± 3
PM3T (60 g/L)	128 ± 1	> 3600	36 ± 3	110 ± 1	2100	45 ± 3
PM3T (100 g/L)	123 ± 1	-	32 ± 2	114 ± 1	-	47 ± 2
$PM3T_{75}SMA_{25}$ (40 g/L)	126 ± 1	-	42 ± 3	115 ± 1	-	43 ± 4
$PM3T_{75}SMA_{25}$ (60 g/L)	127 ± 2	> 3600	47 ± 2	120 ± 1	720	42 ± 4
$PM3T_{75}SMA_{25}$ (100 g/L)	129 ± 2	-	39 ± 5	116 ± 1	-	43 ± 3
$PM3T_{50}SMA_{50}$ (60 g/L)	133 ± 1	> 3600	41 ± 3	120 ± 1	100	48 ± 3
$PM3T_{25}SMA_{75}$ (60 g/L)	129 ± 1	> 3600	45 ± 2	117 ± 3	45	48 ± 3
PSMA (60 g/L)	130 ± 3	> 3600	42 ± 2	absorbed	0	absorbed
C6 PS (60 g/L)	132 ± 1	> 3600	27 ± 3	122 ± 2	> 3600	40 ± 3

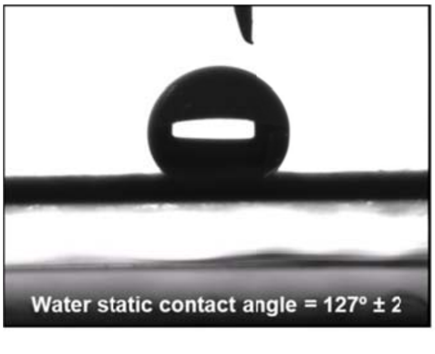

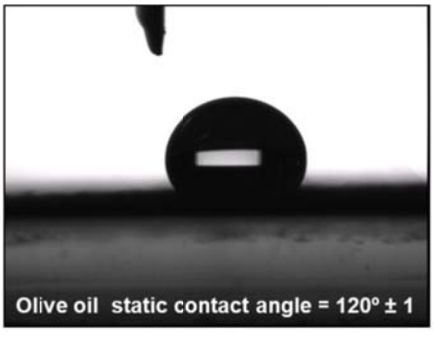

Figure 11. Image of a drop of: a) water and b) olive oil on cotton textile coated with $PM3T_{75}SMA_{25}$ at 60 g/L

To better understand the role of copolymethacrylate's composition on WCA and OCA measurements, a control experiment applying these products on smooth glass slides was carried out. The surface free energy of the coated surfaces has been measured showing that PM3T has a surface free energy (around 21 mN/m) whereas the surface free energy of the PSMA is higher (around 26 mN/m). The surface energy of copolymethacrylates are even lower and only slightly higher than the slide covered with the C6 fluoropolymer. These values are in good agreement with previous results [2], but in our study the surface free energy of the polyacrylates is lower than previous reported values due to the different chemical structure.

During the contact angle measurements, a decrease with time of the initial olive oil's contact angle on some glass slide surfaces has been observed. The Table 10 collects the surface free energies calculated from deionized water and olive oil contact angles obtained at time 0, 2, 10, 30 and 60 min. Values at time 0 are in good agreement with the values obtained by Lei et al. for M3T containing copolymethacrylates [2]. For the coatings with higher M3T content, the surface free energy remains constant with time, whereas the coatings with higher SMA content undergo an increase with time. At the molecular level, this trend can be reasoned on the basis that, as the SMA content increases in the coating, the stearyl side chains once in contact with the olive oil reorient themselves over time due to the Van der Waals interactions with the oil. Moreover, the reduction in M3T content causes an increase in the distance between bulky tris(trimethylsilyloxy)silyl side chains, thus reducing the barrier protection of the coating to olive oil.

Table 10. Evolution of surface free energies with time for the coatings applied on glass slides

	Surface free energy (mN/m)				
	t = 0 min	t = 2 min	t = 10 min	t = 30 min	t = 60 min
PM3T (60 g/L)	21.5	22.2	22.3	22.6	22.1
$PM3T_{75}SMA_{25}$ (60 g/L)	16.4	15.9	18.7	15.9	15.8
$PM3T_{50}SMA_{50}$ (60 g/L)	14.3	17.8	22.4	25.0	26.4
$PM3T_{25}SMA_{75}$ (60 g/L)	16.2	18.8	21.4	22.0	22.4
PSMA (60 g/L)	26.0	26.8	26.9	33.1	32.7
C6 PS (60 g/L)	13.4	13.5	13.6	13.3	13.4

In the case of the coated cotton fabrics, significant differences are observed in the time that the droplets of olive oil remain on fabric's surfaces, due to the coating composition. Whereas the olive oil is immediately absorbed by the fabric coated with PSMA, the olive oil droplet remains initially on the surface of the fabrics with copolymethacrylates and PM3T and thereafter, it is progressively absorbed. This can be related to the evolution of the surface free energy of the product. The time that an olive droplet remains on the surface increases with M3T content, reaching a maximum around 2100 s for the M3T homopolymer. The tilt angle for water and olive oil is quite similar for all the samples but higher than C6 PS fluorocarbon, indicating the higher surface free energy of cotton fabrics treated with $PM3T_xSMA_y$ emulsions, as previously observed in Table 9. Moreover, for the three doses of PM3T and $PM3T_{75}SMA_{25}$ finishing agent that have been applied on cotton fibres, only slight changes in static and tilt angle measurements for water and oil were observed. It can be concluded that 60 g/L is an optimum dosage and dosages of 100 g/L do not lead to better results.

Overall, the coatings showed good hydrophobicity but limited oleophobic properties, as olive oil drops remained on the surfaces and thereafter, they soaked. The best results in terms of oleo-repellence are obtained for PM3T and $PM3T_{75}SMA_{25}$, while PSMA presented the worse results. However, it is important to highlight that $PM3T_xSMA_y$ emulsions are able to confer oil-repellence against fatty triglycerides without using fluorine, this paves the way for the use of these new polymers for different applications, such as anti-stain finishing and solvent-water separation.

The anti-stain performance of $PM3T_xSMA_y$ emulsions is shown in Table 11, Table 12 and Table 13. For untreated cotton, all the liquids quickly spread and penetrated, leaving a marked stain after removing the liquid and cleaning the substrate. However, the cotton substrates coated with $PM3T_xSMA_y$ emulsions at 60 g/L retain the drop of water-based liquids on the surface for 5 min and much longer time. Moreover, the drop of olive oil is also maintained on the surface for PM3T and $PM3T_{75}SMA_{25}$ for 5 min (thereafter, drop soaked). After carefully removing the remaining drop, it can be observed that drops of liquids with higher surface tensions, such as water, coffee and juice + milk drops, do not leave any mark on textiles. Wine left a small mark on all surfaces, even in the C6 fluorocarboned substrate. Finally, the drop of liquid with the lowest surface tension, the olive oil, left a noticeable mark on textiles which have absorbed the drop, but only a slight mark is observed for PM3T coated textile and the mark on $PM3T_{75}SMA_{25}$ coated textile is almost undetectable. As it was expected the oil repellence of the textiles increases with the M3T content in copolymer.

Table 11. Image of a drop of liquid after 5 min. on untreated and coated cotton textiles

<table>
<tr><th>Anti-stain performance</th><th>water</th><th>coffee</th><th>red wine</th><th>Juice + milk</th><th>Olive oil</th></tr>
<tr><td>Untreated fabric</td><td colspan="5"></td></tr>
<tr><td>PM3T
(60 g/L)</td><td colspan="5"></td></tr>
<tr><td>$PM3T_{75}SMA_{25}$
(60 g/L)</td><td colspan="5"></td></tr>
<tr><td>$PM3T_{50}SMA_{50}$
(60 g/L)</td><td colspan="5"></td></tr>
<tr><td>$PM3T_{25}SMA_{75}$
(60 g/L)</td><td colspan="5"></td></tr>
<tr><td>PSMA
(60 g/L)</td><td colspan="5"></td></tr>
<tr><td>C6 PS
(60 g/L)</td><td colspan="5"></td></tr>
</table>

Table 12. Image of drop residues after cleaning (zenith view) on pristine and coated cotton textiles

<table>
<tr><th>Anti-stain performance</th><th>water</th><th>coffee</th><th>red wine</th><th>Juice + milk</th><th>Olive oil</th></tr>
<tr><td>Untreated fabric</td><td colspan="5"></td></tr>
<tr><td>PM3T
(60 g/L)</td><td colspan="5"></td></tr>
<tr><td>$\text{PM3T}_{75}\text{SMA}_{25}$
(60 g/L)</td><td colspan="5"></td></tr>
<tr><td>$\text{PM3T}_{50}\text{SMA}_{50}$
(60 g/L)</td><td colspan="5"></td></tr>
<tr><td>$\text{PM3T}_{25}\text{SMA}_{75}$
(60 g/L)</td><td colspan="5"></td></tr>
<tr><td>PSMA
(60 g/L)</td><td colspan="5"></td></tr>
<tr><td>C6 PS
(60 g/L)</td><td colspan="5"></td></tr>
</table>

Table 13. Values of drop residues on untreated and coated cotton textiles after 5 min

Anti-stain performance	water	coffee	red wine	Juice + milk	Olive oil
Untreated fabric	0	0	0	0	0
PM3T (60 g/L)	4	4	3	4	2
$\text{PM3T}_{75}\text{SMA}_{25}$ (60 g/L)	4	4	3	4	1
$\text{PM3T}_{50}\text{SMA}_{50}$ (60 g/L)	4	3	2	4	0
$\text{PM3T}_{25}\text{SMA}_{75}$ (60 g/L)	4	3	2	4	0

PSMA(60 g/L)	4	3	2	4	0
C6 PS (60 g/L)	4	4	3	4	4

The solvent-water separation performance of the treated fabrics was validated by a filtering process of a mixture of two immiscible liquids with different surface tensions: water and chloroform in a weight ratio of 1:1 [46,47]. The chloroform-water mixture was slowly poured into the filtration equipment where the treated fabric is already placed and acts as a filtration membrane. Because of its higher density, chloroform comes immediately into contact with the fabric membrane and passes throughout it while water is retained. The filtration process is very fast and it takes less than 30 seconds for all the experiments. The hydrophobic fabrics have been reused 10 times. The mass of water has been weighted after each cycle. As it can be observed in Figure *12*, the water amount remained almost constant for the filtration recycling processes for all the textiles indicating their high efficiency in chloroform-water separation. A video has been included in supporting information showing the performance of a cotton fabric coated with PM3T$_{75}$SMA$_{25}$ at 60 g/L (see Video1).

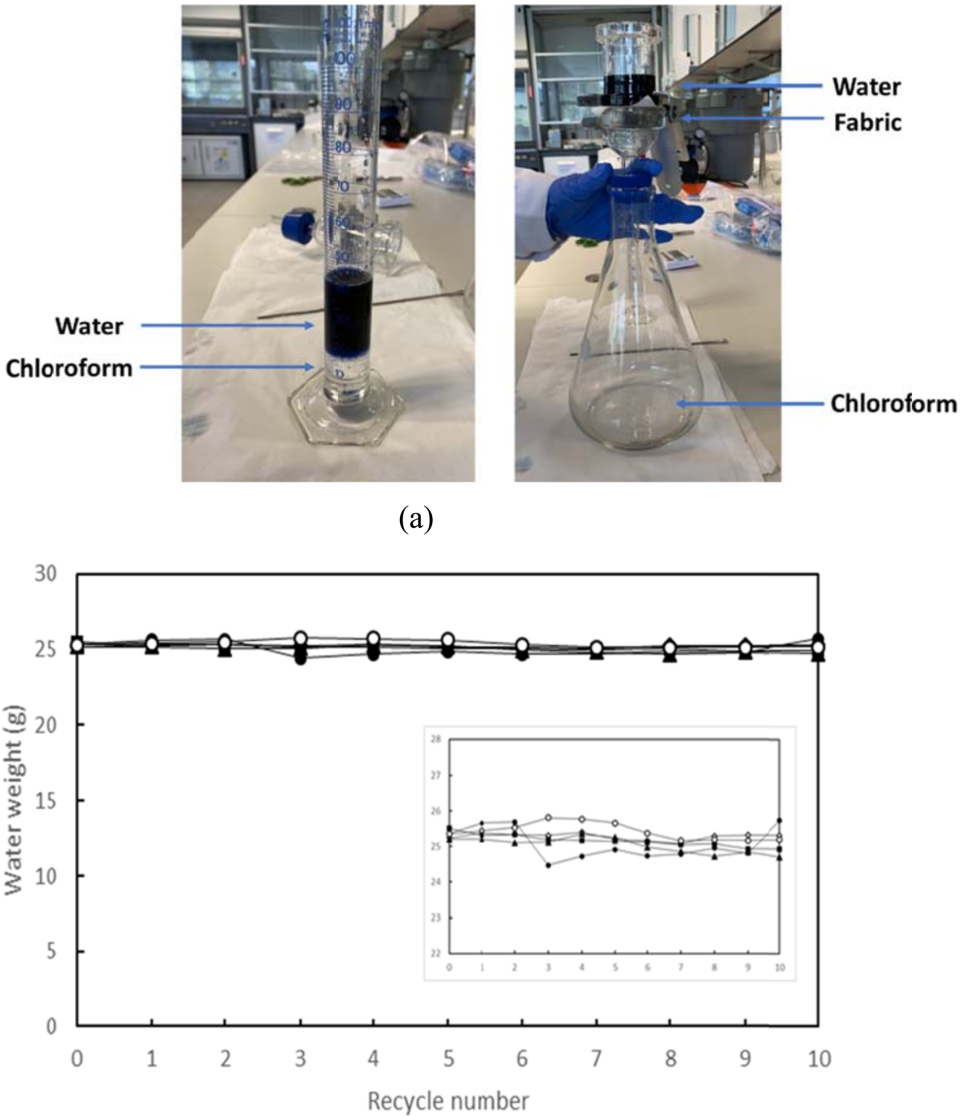

(a)

(b)

Figure 12. (a) Pictures of the chloroform-water separation process and (b) variation of the water weight after each filtering cycle for (●) PM3T, (■) $PM3T_{75}SMA_{25}$, (▲) $PM3T_{50}SMA_{50}$, (○) $PM3T_{25}SMA_{75}$ and (◊) PSMA

Moreover, the fabrics have been also employed for solvent-water separation employing a mixture of n-hexadecane/water in a weight ratio 3:1. The fabrics were employed to prepare a bag in which pristine polyurethane (PU) sponges were filled to achieve high oil absorption capacity (Figure 13) [48]. The weight of water was measured after the separation process showing that all n-hexadecane has been absorbed by the bags. A n-hexadecane:water separation performance between 95 and 98 % has been achieved for all the textiles (*Table 14*).

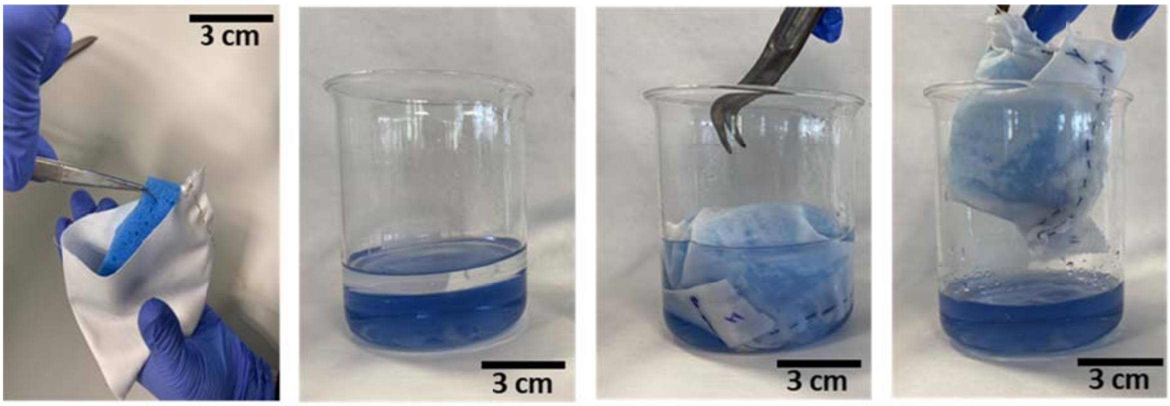

Figure 13. Pictures of the textile during the n-hexadecane-water separation process for the textile treated with $PM3T_{75}SMA_{25}$

Table 14. Effiency of n-hexadecane:water separation of the different textiles

n-hexadecane:water separation efficiency	water initial weight (g)	water final weight (g)	Efficiency (%)
PM3T (60 g/L)	60.1	57.9	96.3
$PM3T_{75}SMA_{25}$ (60 g/L)	62.9	61.2	97.3
$PM3T_{50}SMA_{50}$ (60 g/L)	60.1	57.5	95.7
$PM3T_{25}SMA_{75}$ (60 g/L)	60.1	58.9	98.0
PSMA (60 g/L)	60.6	58.3	96.2

Finally, air permeability, tensile strength and elongation of some of the finished cotton fabrics were measured and compared with the values from the untreated fabric. As can be seen in Table 15, the cotton fabrics finished with 60g/L of PM3T and $PM3T_{75}SMA_{25}$ does not result in significant change of air permeability, tensile strength and elongation with respect to the untreated fabric.

Table 15. Air permeability, tensile strength and elongation of untreated and treated fabrics with PM3T and $PM3T_{75}SMA_{25}$

	Untreated fabric	PM3T	$PM3T_{75}SMA_{25}$

		(60 g/L)	(60 g/L)
Air permeability (mm/s)	119	112	111
Tensile strength (N)	warp: 1039 weft: 544	warp: 1045 weft: 589	warp: 1073 weft: 570
Elongation (%)	warp: 15.3 weft: 13.4	warp: 15.7 weft: 14.0	warp: 15.6 weft: 14.3

3. Conclusions

A series of waterborne $PM3T_xSMA_y$ emulsions have been successfully synthesized by emulsion free radical polymerization of M3T and SMA, being the latter a bio-based monomer, with the aim of obtaining eco-friendly WOR finishing agents for textile applications. Monomer conversion was qualitatively assessed by FTIR and chemical structure, tacticity and copolymer composition was studied by NMR. DSC results corroborated the random polymerization of the comonomers as well as first and second order thermal transitions, whereas EDS confirmed an increasing content of silicon with the increase of M3T in the obtained copolymers. TGA was used to determine the thermal stability of the (co)polymers. Moreover, particle size, particle size distribution and zeta potential of the (co)polymethacrylate emulsions have been analysed. The results showed that (co)polymethacrylate emulsions had good stability, all of them showing a particle size below 200 nm (d(50)) as well as narrow unimodal particle size distribution.

Thereafter, the $PM3T_xSMA_y$ emulsions were applied onto cotton fabric by padding method and the textile surface and performance were then characterized and compared against conventional C6 fluorocarbon. SEM and XRF analysis confirmed that (co)polymethacrylates had been successfully applied onto the surface of cotton fabric. As expected, a decreasing content of elemental silicon is observed in the textiles with the decrease of M3T molar ratio in the copolymer. EDS mapping analysis of silicon indicated a homogeneous distribution of the finishing agents on the fabric's surface. Static contact angle measurements, WCA and OCA, showed that all the studied finishing agents provided cotton with good hydrophobicity with WCA around 127-133º, and acceptable oleophobic properties in front of olive oil. OCA between 101º and 120º were obtained for all the treated substrates except for the fabrics treated with PSMA where olive oil soaked immediately due to the absence of tris-trimethylsilyl functional groups. Olive oil's drops only remained on the fabrics' surface for a limited period (from a few seconds for (co)polymers with low M3T content to several minutes for (co)polymers with higher M3T ratio) and thereafter they soaked. This time-dependent wettability may be ascribed to the evolution with time of the surface free energy of the coatings with lower M3T contents due to a reorientation over time of stearyl side chains of SMA once in contact with the olive oil and to the lower barrier properties of the coatings with lower contents of the bulky tris-trimethylsilyl side-chains.

In any case, it is important to highlight that $PM3T_xSMA_y$ emulsions can confer oil-repellence against fatty triglycerides without using fluorinated chemicals, neither VOCs or harmful chemicals, which is a remarkable achievement. XRF and SEM micrographs, as well as WCA and OCA, were very useful to determine the optimum dosage of WOR finishing agents in the padding liquor and therefore on the fabrics, indicating that doses of 60 g/L or lower are optimum for the selected fabrics. Anti-staining properties of the treated fabrics against liquids of watery or oily nature were also studied. $PM3T_xSMA_y$

emulsions with highest M3T content proved to be the most efficient as anti-staining agents, especially for olive oil. This can be ascribed to the low surface energy conferred by M3T functional groups. The excellent performance of all the treated textiles as solvent-water separation membrane has also been demonstrated for separation of chloroform:water mixtures and n-hexadecane:water mixtures. For this specific application, the key factor is to provide the treated fabrics with high hydrophobicity, which can be conferred either by the SMA saturated fatty chains or by the tris-trimethylsilyl groups from the M3T (co)monomer. Finally, some valuable physical-mechanical parameters of the untreated fabric like air permeability, tensile strength and elongation are not significantly altered in the coated fabrics, showing values very similar to those of the untreated fabric.

Therefore, the fluorine-free finishing agents based on waterborne emulsions of tris-trimethylsilyl and stearyl (co)polymethacrylates will contribute to lower the environmental impact of WOR finishing processes in the textile industry and solvent-water separation sector. In view of these promising results and the urgent need for replacement of fluorochemicals, which are known for bioaccumulation and persistence in the environment, more efforts should be devoted to the design of new polymers based on fluorine-free building blocks that provide advanced surface properties.

Acknowledgments

This work under “E!11894 ECO-DWOR” project (CIIP-20181001) is supported by the European Union under the Eurostars Programme in cooperation with CDTI (Centro para el Desarrollo Tecnológico Industrial) as operator in Spain. Additional financial support received from the AGAUR (Doctorats Industrials: 2018 DI 093) is also gratefully acknowledged. We want to thank Lenka Martinková from INOTEX spol. s r.o. for her contribution in characterization of physical-mechanical properties of fabrics.

Tables

Figure Captions

Figure 1. Long-term wettability of the textiles treated with C8, C6 and C4 fluorocarbons. Adapted from ref. [1]
Figure 2. Chemical structure of: a) SMA and b) M3T monomers
Figure 3. FTIR spectra in the MIR region for $PM3T_{50}SMA_{50}$ sample before (top, green) and after polymerization (bottom, black)
Figure 4. ^1H NMR (top) and ^{13}C NMR (bottom) spectra of $PM3T_{50}SMA_{50}$ with peak assignments
Figure 5. Expanded ^{13}C NMR spectra of PM3T, PSMA and M3T-containing copolymethacrylates in the region of the main chain CH_2 (3,3'), C (2,2') and CH_3 (1,1') carbons with peak assignments to different stereosequences
Figure 6. Second heating (a) and cooling (b) DSC thermograms of the methacrylic (co)polymer. From top to bottom PSMA, $PM3T_{25}SMA_{75}$, $PM3T_{50}SMA_{50}$, $PM3T_{75}SMA_{25}$, PM3T.
Figure 7. Particle size distribution obtained by LDS for: a) $PM3T_{50}SMA_{50}$ and b) reference C6 fluorocarbon
Figure 8. SEM micrographs for: (a) untreated cotton and coated cotton fabrics: (b) PM3T, (c) $PM3T_{75}SMA_{25}$, (d) $PM3T_{50}SMA_{50}$, (e) $PM3T_{25}SMA_{75}$, (f) PSMA and (g) C6 PS with a dosage of 60 g/L. Micrographs have been obtained with a magnification of x2000 and 3.3 mm of working distance
Figure 9. SEM micrographs for PM3T and $PM3T_{75}SMA_{25}$ coated cotton textiles with a dosage of 40, 60 and 100 g/L. Micrographs have been obtained with a magnification of x2000 and 3.3 mm of working distance
Figure 10. EDS mapping of coated cotton textiles with doses of 60 g/L of: a) $PM3T_{75}SMA_{25}$ emulsion (silicon in red) and b) C6 PS fluorocarbon (fluorine in green and chlorine in red)
Figure 11. Image of a drop of: a) water and b) olive oil on cotton textile coated with $PM3T_{75}SMA_{25}$ at 60 g/L
Figure 12. (a) Pictures of the chloroform-water separation process and (b) variation of the water weight after each filtering cycle for (●) PM3T, (■) $PM3T_{75}SMA_{25}$, (▲) $PM3T_{50}SMA_{50}$, (○) $PM3T_{25}SMA_{75}$ and (◊) PSMA
Figure 13. (a) Pictures of the textile during the n-hexadecane-water separation process for the textile treated with $PM3T_{75}SMA_{25}$

Data availability statement

The raw/processed data required to reproduce these findings cannot be shared at this time as the data also forms part of an ongoing study.

References

[1] M. Zahid, G. Mazzon, A. Athanassiou, I. S. Bayer, Environmentally benign non-wettable textile treatments: A review of recent state-of-the-art, Adv. Colloid Interface Sci. 270 (2019) 216–250. https://doi.org/10.1016/j.cis.2019.06.001.
[2] H. Lei, M. Xiong, J. Xiao, L. Zheng, Y. Zhu, X. Li, Q. Zhuang, Z. Han, Fluorine-free low surface energy organic coating for anti-stain applications, Prog. Org. Coat. 103 (2017) 182–192. https://doi.org/10.1016/j.porgcoat.2018.07.036.

[3] M. Ma, Y. Mao, M. Gupta, K.K. Gleason, G.C. Rutledge, Superhydrophobic fabrics produced by electrospinning and chemical vapor deposition, Macromolecules 38 (2005) 9742–9748. https://doi.org/10.1021/ma0511189.

[4] D. Xiong, G. Liu, E.J.S. Duncan, Diblock-copolymer-coated water-and oil-repellent cotton Fabrics, Langmuir 28 (2012) 6911–6918. https://doi.org/10.1021/la300634v.

[5] GORE-TEX garment technology, GORE-TEX brand. https://www.gore-tex.com/technology/original-gore-tex-products/garments.

[6] J.W. Martin, S.A. Mabury, K.R. Solomon, D.C.G. Muir, Progress toward understanding the bioaccumulation of perfluorinated alkyl acids, Environ. Toxicol. Chem. 32 (2013) 2421–2423. https://doi.org/10.1002/etc.2376.

[7] B.J. Apelberg, F.R. Witter, J.B. Herbstman, A.M. Calafat, R.U. Halden, L.L. Needham, L.R. Goldman, Cord serum concentrations of perfluorooctane sulfonate (PFOS) and perfluorooctanoate (PFOA) in relation to weight and size at birth, Environ. Health Perspect. 115 (2007) 1670–1676. https://doi.org/10.1289/ehp.10334.

[8] C. Fei, J.K. McLaughlin, R.E. Tarone, J. Olsen, Perfluorinated chemicals and fetal growth: A study within the Danish national birth cohort, Environ. Health Perspect. 115 (2007) 1677–1682. https://doi.org/10.1289/ehp.10506.

[9] L. Vierke, C. Staude, A. Biegel-Engler, W. Drost, C. Schulte, Perfluorooctanoic acid (PFOA)-main concerns and regulatory developments in Europe from an environmental point of view, Environ. Sci. Eur. 24 (2012) 16. https://doi.org/10.1186/2190-4715-24-16.

[10] K.J. Hansen, L.A. Clemen, M.E. Ellefson, H.O. Johnson, Compound-specific, quantitative characterization of organic fluorochemicals in biological matrices, Environ. Sci. Technol. 35 (2001) 766–770. https://doi.org/10.1021/es001489z.

[11] B. Ballarin, D. Barreca, M.C. Cassani, G. Carraro, C. Maccato, A. Mignanii, D. Lazzari, M. Bertola, Fluoroalkylsilanes with embedded functional groups as building blocks for environmentally safer self-assembled monolayers, Langmuir 31 (2015) 6988–6994. https://doi.org/10.1021/acs.langmuir.5b01416.

[12] S. Nagappan, M.C. Choi, G. Sung, W.K. Lee, C.S. Ha, Highly transparent, hydrophobic fluorinated polymethylsiloxane/silica organic-inorganic hybrids for anti-stain coating, Macromol. Res. 21 (2013) 669–680. https://doi.org/10.1007/s13233-013-1069-7.

[13] E. Bormashenko, R. Grynyov, G. Chaniel, H. Taitelbaum, Y. Bormashenko, Robust technique allowing manufacturing superoleophobic surfaces, Appl. Surf. Sci. 270 (2013) 98–103. https://doi.org/10.1016/j.apsusc.2012.12.124.

[14] J. Williams, Waterproof and water repellent textiles and clothing, first ed., Elsevier Inc., 2017. https://doi.org/10.1016/C2015-0-06037-3.

[15] A.L. Luz, J.K. Anderson, P. Goodrum, J. Durda, Perfluorohexanoic acid toxicity, part I: Development of a chronic human health toxicity value for use in risk assessment, Regul. Toxicol. Pharmacol. 103 (2019) 41–55. https://doi.org/10.1016/j.yrtph.2019.01.019.

[16] J.E. Klaunig, M. Shinohara, H. Iwai, C.P. Chengelis, J.B. Kirkpatrick, Z. Wang, R.H. Bruner, Evaluation of the chronic toxicity and carcinogenicity of perfluorohexanoic acid (PFHxA) in Sprague-Dawley Rats, Toxicol. Pathol. 43 (2015) 209–220. https://doi.org/10.1177/0192623314530532.

[17] Y. Liu, Y. Liu, H. Hu, Z. Liu, X. Pei, B. Yu, P. Yan, f. Zhou, Mechanically induced self-healing superhydrophobicity, J. Phys. Chem. C. 119 (2015) 7109–14. https://doi.org/10.1021/jp5120493.

[18] K. Sasaki, M. Tenjimbayashi, K. Manabe, S. Shiratori, Asymmetric superhydrophobic/superhydrophilic cotton fabrics designed by spraying polymer and

nanoparticles, ACS Appl. Mater. Interfaces 8 (2016) 651-659. https://doi.org/10.1021/acsami.5b09782.

[19] N.F. Attia, M. Moussa, A.M.F. Sheta, R. Taha, H. Gamal, Effect of different nanoparticles based coating on the performance of textile properties, Prog. Org. Coat. 104 (2017) 72–80. https://doi.org/10.1016/j.porgcoat.2016.12.007.

[20] T. Kim, H. Kang, N. Yoon, Synthesis of non-fluorinated paraffinic water repellents and application properties on textile fabrics, Fibers Polym. 18 (2017) 285-289. https://doi.org/10.1007/s12221-017-6469-4.

[21] Q. Zhu, Q. Gao, Y. Guo, C.Q. Yang, L. Shen, Modified silica sol coatings for highly hydrophobic cotton and polyester fabrics using a one-step procedure, Ind. Eng. Chem. Res. 50 (2011) 5881-5888. https://doi.org/10.1021/ie101825d.

[22] M. Zahid, J.A. Heredia-Guerrero, A. Athanassiou, I.S. Bayer, Robust water repellent treatment for woven cotton fabrics with eco-friendly polymers, Chem. Eng. J. 319 (2017) 321-332. https://doi.org/10.1016/j.cej.2017.03.006.

[23] D. Chen, F. Chen, H. Zhang, X. Yin, Y. Zhou, Preparation and characterization of novel hydrophobic cellulose fabrics with polyvinylsilsesquioxane functional coatings, Cellulose 23 (2016) 941-953. https://doi.org/10.1007/s10570-015-0820-y.

[24] Y. Wu, H. Qi, B. Li, Z. Huang, W. Li, S. Liu, Novel hydrophobic cotton fibers adsorbent for the removal of nitrobenzene in aqueous solution, Carbohydr. Polym. 155 (2017) 294-302. https://doi.org/10.1016/j.carbpol.2016.08.088.

[25] J. Li, L. Yan, Y. Zhao, F. Zha, Q. Wang, Z. Lei. One-step fabrication of robust fabrics with both-faced superhydrophobicity for the separation and capture of oil from water. Phys. Chem. Chem. Phys. 17 (2015) 6451-6457. https://doi.org/10.1039/c5cp00154d.

[26] N. Guo, Y. Chen, Q. Rao, Y. Yin, C. Wang, Fabrication of durable hydrophobic cellulose surface from silane-functionalized silica hydrosol via electrochemically assisted deposition, J. Appl. Polym. Sci. 132 (2015) 42733–42739. https://doi.org/10.1002/app.42733.

[27] Q. Liu, J. Huang, J. Zhang, Y. Hong, Y. Wan, Q. Wang, m. Gong, Z. Wu, C.F. Guo, Thermal, waterproof, breathable, and antibacterial cloth with a nanoporous structure, ACS Appl. Mater. Interfaces 10 (2018) 2026–2032. https://doi.org/10.1021/acsami.7b16422.

[28] S. Xu, H. Li, X. Lai, L. Zhang, J. Wang, X.F. Liao, X.R. Zeng, Vapor-liquid sol-gel approach to fabricating highly durable and robust superhydrophobic polydimethylsiloxane@silica surface on polyester textile for oil-water separation, ACS Appl. Mater. Interfaces 9 (2017) 28089–28099. https://doi.org/10.1021/acsami.7b08920.

[29] H. Wang, H. Zhou, S. Liu, H. Shao, S. Fu, G.C. Rutledge, T. Lin, Durable, self-healing, superhydrophobic fabrics from fluorine-free, waterborne, polydopamine/alkyl silane coatings, RSC Adv. 7 (2017) 33986–33993. https://doi.org/10.1039/c7ra04863g.

[30] S. Fu, H. Zhou, H. Wang, J. Ding, S. Liu, Y. Zhao, H. Niu, G.C. Rutledge, T. Lin, Magnet-responsive, superhydrophobic fabrics from waterborne, fluoride-free coatings. RSC Adv. 8 2018) 717–723. https://doi.org/10.1039/c7ra10941e.

[31] Y. Yin, R. Huang, W. Zhang, M. Zhang, C. Wang, Superhydrophobic-superhydrophilic switchable wettability via TiO2 photoinduction electrochemical deposition on cellulose substrate, Chem. Eng. J. 289 (2016) 99-105. https://doi.org/10.1016/j.cej.2015.12.049.

[32] D. Zhang, B.L. Williams, S.B. Shrestha, Z. Nasir, E.M. Becher, B.J. Lofink, V.H. Santos, H. Patel, X. Peng, L. Sun, Flame retardant and hydrophobic coatings on cotton fabrics via sol-gel and self-assembly techniques, J. Colloid Interface Sci. 505 (2017)

892–899. https://doi.org/10.1016/j.jcis.2017.06.087.

[33] N.D. Tissera, R.N. Wijesena, J.R. Perera, K.M.N. de Silva. G.A.J. Amaratunge, Hydrophobic cotton textile surfaces using an amphiphilic graphene oxide (GO) coating, Appl. Surf. Sci. 324 (2015) 455–463. https://doi.org/10.1016/j.apsusc.2014.10.148.

[34] J.H. Oh, T.J. Ko, M.W. Moon, C.H. Park, Nanostructured fabric with robust superhydrophobicity induced by a thermal hydrophobic ageing process, RSC Adv. 7 (2017) 25597–25604. https://doi.org/10.1039/c7ra03801a.

[35] M. Zhang, J. Pang, W. Bao, W. Zhang, H. Gao, C. Wang, J. Shi, J. Li, Antimicrobial cotton textiles with robust superhydrophobicity via plasma for oily water separation, Appl. Surf. Sci. 419 (2017) 16–23. https://doi.org/10.1016/j.apsusc.2017.05.008.

[36] J. Zhang, Z. Gao, L. Li, B. Li, H. Sun, Waterborne nonfluorinated superhydrophobic coatings with exceptional mechanical durability based on natural nanorods, Adv. Mater. Interfaces 4 (2017) 1700723. https://doi.org/10.1002/admi.201700723.

[37] H. Ye, L. Zhu, W. Li, H. Liu, H. Chen, Simple spray deposition of a water-based superhydrophobic coating with high stability for flexible applications, J. Mater. Chem. A 5 (2017) 9882–9890. https://doi.org/10.1039/C7TA02118F.

[38] X. Zhao, Y. Li, B. Li, T. Hu, Y. Yang, L. Li, J. Zhang, Environmentally benign and durable superhydrophobic coatings based on SiO2 nanoparticles and silanes, J. Colloid Interface Sci. 542 (2019) 8–14. https://doi.org/10.1016/j.jcis.2019.01.115.

[39] W.K. Owens, R.C. Went, Estimation of the surface free energy of polymers, J. Appl. Polymer Sci. 13 (1969) 1741-1747. https://doi.org/10.1002/app.1969.0701130815.

[40] D. Saha, M. Hait, M. Patanwar, Ankit Tamrakar, Studies on surface tension of selected juice formulation by drop number method using Traube’s stalagmometer technique, Bull.Pharm. Res 1 (2011) 1-3. https://doi.org/10.13140/RG.2.1.1864.0080

[41] R. Chandan, Dairy Based Ingredients: Practical Guides for the Food Industry, Eagen Press Handbook Series, USA (1997).

[42] L. Navarini, M. Ferrari, F. S. Liverani, L. Liggieri, F. Ravera, Dynamic tensiometric characterization of espresso coffee beverage, Food Hydrocolloids 18 (2004) 387–393. https://doi.org/10.1016/S0268-005X(03)00126-7

[43] P. Glampedaki, E. Hatzidimitriou, A. Paraskevopoulou, S. Pegiadou-Koemtzopoulou, Surface tension of still wines in relation to some of their constituents: A simple determination of ethanol content, J Food Comp Anal 23 (2010) 373-381. https://doi.org/10.1016/j.jfca.2010.01.006

[44] Y. Sun, X. Zhao, R. Liu, G. Chen, X. Zhou, Synthesis and characterization of fluorinated polyacrylate as water and oil repellent and soil release finishing agent for polyester fabric, Prog. Org. Coat. 123 (2018) 306–313. https://doi.org/10.1016/j.porgcoat.2018.07.013.

[45] Q. An, W. Xu, L. Hao, L. Huang, Cationic fluorinated polyacrylate core-shell latex with pendant long chain alkyl: synthesis, film morphology, and its performance on cotton substrates, J. Appl. Polym. Sci. 127 (2013) 1519–1526. https://doi.org/10.1002/app.37553.

[46] X. Dong, S. Gao, J. Huang, S. Li, T. Zhu, Y. Cheng, Y. Lai, A self-roughened and biodegradable superhydrophobic coating with UV shielding, solar-induced self-healing and versatile oil-water separation ability. J. Mat. Chem. A 7 (2019) 2122-2128. https://doi:10.1039/c8ta10869b

[47] Y. Deng, D. Han, Y.Y. Deng, Q. Zhang, O. Fu, Facile one-step preparation of robust hydrophobic cotton fabrics by covalent bonding polyhedral oligomeric

silsesquioxane for ultrafast oil/water separation, Chem. Eng. J. 379 (2020) 122391. https://doi.org/10.1016/j.cej.2019.122391

[48] C. Cao, M. Ge, J. Huang, S. Li, S. Deng, S. Zhang, Y. Lai, Robust fluorine-free superhydrophobic PDMS–ormosil@fabrics for highly effective self-cleaning and efficient oil–water separation. J. Mat. Chem. A 4 (2016) 12179–12187. https://doi:10.1039/c6ta04420d